haematologica
Journal of the Ferrata Storti Foundation

Umbilical cord blood T cells can be isolated and enriched by CD62L selection for use in 'off the shelf' chimeric antigen receptor T-cell therapies to widen transplant options

by Christos Georgiadis, Lauren Nickolay, Farhatullah Syed, Hong Zhan, Soragia Athina Gkazi, Annie Etuk, Ulrike Abramowski-Mock, Roland Preece, Piotr Cuber, Stuart Adams, Giorgio Ottaviano, and Waseem Qasim

Received: Jan 20, 2024.
Accepted: July 3, 2024.

Citation: Christos Georgiadis, Lauren Nickolay, Farhatullah Syed, Hong Zhan, Soragia Athina Gkazi, Annie Etuk, Ulrike Abramowski-Mock, Roland Preece, Piotr Cuber, Stuart Adams, Giorgio Ottaviano, and Waseem Qasim. Umbilical cord blood T cells can be isolated and enriched by CD62L selection for use in 'off the shelf' chimeric antigen receptor T-cell therapies to widen transplant options.
Haematologica. 2024 July 11. doi: 10.3324/haematol.2024.285101 [Epub ahead of print]

Umbilical cord blood T cells can be isolated and enriched by CD62L selection for use in 'off the shelf' chimeric antigen receptor T-cell therapies to widen transplant options

Christos Georgiadis[1], Lauren Nickolay[1], Farhatullah Syed[1], Hong Zhan[1], Soragia Athina Gkazi[1], Annie Etuk[1], Ulrike Abramowski-Mock[1], Roland Preece[1], Piotr Cuber[1], Stuart Adams[2], Giorgio Ottaviano[1] and Waseem Qasim[1,2]

[1] UCL Great Ormond Street Institute of Child Health, WC1N 1DZ, London, UK

[2] Great Ormond Street Hospital for Children NHS Trust, WC1N 3JH, London, UK

Corresponding author: Waseem Qasim (w.qasim@ucl.ac.uk)

Running title: Universal CD62L-selected UCB-CAR T cells

Funding

Supported by National Institute of Health Research (NIHR) and Great Ormond Street Biomedical Research Centre (RP-2014-05-007), BRC (IS- BRC-1215-20012) and Children with Cancer (2014/171) and supported by the Medical Research Council MR/X004619/1 and MRC Developmental pathway funding scheme (DPFS). The views expressed are those of the author(s) and not necessarily those of the NHS, the NIHR or the Department of Health.

Disclosures

W.Q., C.G., R.P., A.S.G., and A.E.: UCLB has filed intellectual property in relation to therapeutic cells (WO/2018/115887; PCT/GB2017/053862) and U6 minimal promoter (WO/ 2020/183197; PCT/GB2020/050651). U.A.M. is a current employee of Miltenyi Biotec B.V. & Co. KG. W.Q. has consulted for Wugen, Novartis, Kite, Autolus, Virocell & Galapagos. All other authors declare that they have no competing interests.

Contributions

W.Q. is the principal investigator. C.G., G.O., L.N., F.S. and W.Q. wrote the first draft of the manuscript. C.G., A.E., R.P., and W.Q. developed the vector configuration and genome editing strategy and performed *in vitro* and *in vivo* phenotypic and functional assays. L.N. and U.A.M. assisted with scalability of the platform. F.S., H.Z., and P.C. manufactured the UCB-TT52CAR19 batches and performed the longitudinal stability tests. S.A.G., and S.A. performed the molecular characterisation of the final product. C.G., G.O., S.A.G., and W.Q.

analysed the data and created the figures of this manuscript. All authors reviewed and approved the manuscript.

Acknowledgements

We would like to thank Ailsa Greppi and Kyle O'Sullivan for their invaluable technical support with *in vivo* studies. Dr. Ayad Eddaudi at the UCL Joint Great Ormond Street Institute of Child Health and Institute of Ophthalmology Flow Cytometry Core Facility, supported by the Great Ormond Street Children's Charity (GOSHCC), grant reference U09822 (October 2007), UCL Capital Equipment Funding, School of Life and Medical Sciences (September 2012), and UK Research and Innovation, grant reference MR/ L012758/1 (March 2014). The Anthony Nolan Trust (803716/ SC038827) for their support and provision of healthy blood donations.

Data sharing statement

All data and protocols associated with this work are present in the paper or the Supplementary Materials. Lentiviral plasmids generated in this study are available upon request from the corresponding author under a material transfer agreement. Raw NGS files were deposited in the NIH BioProject Database (BioProject accession number: PRJNA1061060)

Abstract

Umbilical cord blood (UCB) T cells exhibit distinct naïve ontogenetic profiles and may be an attractive source of starting cells for the production of chimeric antigen receptor (CAR) T cells. Pre-selection of UCB-T cells on the basis of CD62L expression was investigated as part of a machine-based manufacturing process, incorporating lentiviral transduction, CRISPR-Cas9 editing, T-cell expansion and depletion of residual TCR$\alpha\beta$ T cells. This provided stringent mitigation against the risk of graft versus host disease (GVHD), and was combined with simultaneous knockout of CD52 to enable persistence of edited T cells in combination with preparative lymphodepletion using Alemtuzumab. Under compliant manufacturing conditions, two cell banks were generated with high levels of CAR19 expression and minimal carriage of TCR$\alpha\beta$ T cells. Sufficient cells were cryopreserved in dose-banded aliquots at the end of each campaign to treat dozens of potential recipients. Molecular characterisation captured vector integration sites and CRISPR editing signatures and functional studies, including *in vivo* potency studies in humanised mice, confirmed anti-leukaemic activity comparable to peripheral blood-derived universal CAR19 T cells. Machine manufactured UCB derived T cells banks offer an alternative to autologous cell therapies and could help widen access to CAR T cells.

Introduction

Chimeric antigen receptor (CAR) T cells can mediate leukaemic remission in patients that have otherwise failed conventional treatment [1]. Current authorised products are manufactured from autologous peripheral blood lymphocytes derived from steady-state apheresis, and this requires complex logistics, and time for manufacturing and release of products [2]. The quality and fitness of such products is highly dependent on individual patient variables [3]. Alternative allogeneic sources are being investigated as a starting material, including T cells from HLA matched haematopoietic stem cell transplant donors [4, 5], or donor derived virus specific T cells [6] and non-matched genome-edited donor derived T cells [7-10]. The latter have been derived from adult volunteer donors and edited to try and address HLA barriers. Steps have included targeted disruption of TCRαβ expression in combination with HLA class I knockout, alone or in combination with class II inhibition [11-16]. We have previously tested strategies to confer resistance to lymphodepleting serotherapy by editing of CD52 and showed that cells persisted for around four weeks in the presence of Alemtuzumab, sufficient time to mediate leukaemic clearance [8, 9, 17].

Umbilical cord blood (UCB) T cells have distinct ontogenetic origins and may offer enhanced properties of expansion and activation, compared to adult peripheral blood lymphocytes [18]. The specific transcriptional signature of UCB T cells has been affiliated with potent anti-leukaemic effects after allogeneic transplantation [19]. Several groups have explored the efficacy of UCB-derived immune cells modified to express CARs in pre-clinical models, and clinical testing of cord derived natural killer (NK) cells has been underway in patients with B-cell malignancies, with encouraging early data [20-23]. UCB T-cell naivety and high proliferative capacity warrants their further investigation for CAR T cell production [24]. Challenges include the limited volume of UCB collections and their high nucleated red cell and mononuclear cell content which complicates T cell isolation and processing. CD62L is expressed on almost all UCB T cells and we reasoned that selecting for CD62L could allow T cells to be efficiently isolated from umbilical collections. CD62L generally identifies less-differentiated T cells (naïve and central memory T cells) from effector subsets [25, 26] and represents an important homing marker [27]. Importantly, selection by targeting CD62L avoids binding of T-cell receptors or other key activation ligands, and this may be important for downstream activation and transduction steps. T cells are most efficiently transduced while undergoing

mitosis and this is generally best achieved through a combination of anti-CD3 and anti-CD28 antibody stimulation. Previously we generated adult donor CAR19 T cells, with T-cell receptor alpha constant gene (*TRAC*) and *CD52* multiplexed knockouts using lentiviral gene modification of peripheral blood CAR T cells for a Phase I clinical trial in children with refractory/relapsed (R/R) B-ALL [8]. These processes were now adopted for 'compliance-ready' machine manufacture of UCB T cells, starting with CD62L positive selection and ending with TCRαβ negative selection of TCRαβ depleted CAR19 T cells. Molecular, phenotypic and functional assessments were undertaken to determine suitability and feasibility of downstream therapeutic applications.

Methods

Manufacture of UCB-TT52CAR19

Fresh umbilical cord blood units were collected under ethical approval from volunteers identified independently by the Nolan transplant registry and tissue typed at St Barts Hospital National Health System (NHS) Trust. A unit was directly attached to the CliniMACS Prodigy device (Miltenyi Biotec). T cells were enriched by automatic red blood cell depletion and CD62L positive selection. The $CD62L^+$ UCB T cells were then activated using MACS GMP TransAct (Miltenyi Biotec) on a modified T-cell transduction (TCT) program and cultured in TexMACS supplemented with 3% human serum (HS) (Life Science Production) and interleukin-2 (IL-2) (Miltenyi Biotec) for 24 hours. The cells were transduced on device with TT52CAR19 lentiviral vector, previously described [8]. On day 4 post activation, cells were removed from the CliniMACS Prodigy and electroporated with capped, polyadenylated, and uridine modified SpCas9 mRNA using the Lonza 4D-Nucleofector LV unit. Post electroporation, cells were returned to the CliniMACS Prodigy and cultured at 5% CO_2 37°C until day 11 with timed TexMACS supplemented with 3% HS/IL-2. Programmed media changes with shaking enabled for optimal gas exchange. On day 11 cells underwent automatic TCRαβ depletion on the CliniMACS Prodigy using an anti-biotin bead kit. The depleted cells were rested overnight in the device and the final drug substance was harvested on day 12 and cryopreserved in 1×10^7 and 2×10^7 doses. Next Generation Sequencing (NGS) was used for high-resolution tissue typing of UCB1 (HLA-A*02:01:01, -A*24:02:01, HLA-B*07:02:01, -B*15:01:01, HLA-C*03:03:01, -C*07:02:01, HLA-DRB1*01:02:01, -DRB1*15:01:01, HLA-DRB5*01:01:01, HLA-DQB1*05:01:01, -DQB1*06:02:01,

HLA-DPA1*01:03:01, -DPA1*02:01:01, HLA-DPB1*04:01:01, -DPB1*11:01:01, HLA-DQA1*01:01:02, -DQA1*01:02:01) and UCB2 (HLA-A*01:01:01, -A*25:01:01, HLA-B*07:02:01, -B*08:01:01, HLA-C*07:01:01, -C*07:02:01, HLA-DRB1*03:01:01, -DRB1*04:01:01, HLA-DRB3* 01:01:02, HLA-DRB4*01:03:01, HLA-DQB1*02:01:01, -DQB1*03:02:01, HLA-DPA1*01:03:01, HLADPB1*04:01:01, HLA-DQA1*03:01:01, -DQA1*05:01:01) batches **(Table S1)**.

Phenotype, Function and Molecular Characterisation

Flow cytometry

Flow cytometry was undertaken using a BD FACSCanto II (Becton, Dickinson BD Biosciences) at Great Ormond Street Hospital (GOSH) NHS Trust, with additional characterisation using a BD LSRII (Becton, Dickinson BD Biosciences), and analysis using FlowJo v10 (TreeStar Inc.).

Quantification of on- and off-target editing effects and translocations

PCR amplicons of target genomic DNA were Sanger sequenced and non-homologous end joining (NHEJ) events analysed using Inference of CRISPR Edits (ICE) protocols (https://ice.synthego.com/#/). On-target and off-target sites were informed by previous Digenome-seq studies [7, 28] **(Table S2)** and libraries subjected to paired-end NGS using MiniSeq (Illumina) as previously described [29-31]. Droplet digital PCR (ddPCR) was used to quantify predicted translocations between chromosomes 14q (TRAC) and 1p (CD52) loci and analysed using Quantasoft (BioRad) **(Table S2)**. (BioProject accession number: PRJNA1061060)

In vitro cytotoxicity assay

In vitro cytotoxic function of UCB-TT52CAR19 GMP1 (UCB1) and UCB-TT52CAR19 GMP2 (UCB2) or peripheral blood leukapheresis (PBL) derived batches alongside controls was quantified by co-culture with chromium (^{51}Cr) loaded CD19^{+} Daudi and CD19^{+} or CD19^{-} SupT1 cells for 4 hours at 37°C at increasing effector-to-target (E:T) (0.16:1 – 20:1 where a 1:1 E:T used 5 x 10^{4} of each group) ratios and ^{51}Cr release was quantified using a Wallac MicroBeta TriLux microplate scintillation counter.

In vivo studies

In vivo function was assessed in non-obese diabetic (NOD)/severe combined immunodeficiency (SCID)/γc (NSG) mice inoculated intravenously by tail vein injection with 0.5 x 10^6 $CD19^+$ Daudi tumour cells expressing enhanced green fluorescence protein (eGFP) and luciferase, followed by 5 x 10^6 UCB1, UCB2 or PBL derived effectors and non-edited or non-transduced controls after 4 days. Serial bioluminescence imaging using an IVIS Lumina III In Vivo Imaging System (PerkinElmer, Living Image® version 4.5.5) was used to track leukaemia inhibition for up to 4 weeks.

Statistical analysis

Statistical analyses were performed with Prism (GraphPad) using unpaired t test or ANOVA where indicated. Values from 3 or more samples are presented as mean with SEM. $P < 0.05$ was considered significant.

Results

Machine mediated $CD62L^+$ T-cell enrichment and engineering of UCB donations

Banks of UCB-TT52CAR19 (UCB1 and UCB2) were manufactured from two fresh, unrelated volunteer donor, cord blood collections using a CliniMACS Prodigy device **(Figure 1 and Table S1)**. One key hurdle in handling and manipulating UCB donations is the high number of nucleated red cells. We investigated $CD62L^+$ T-cell enrichment by CD62L selection using magnetic bead positive selection. A yield of >4 x 10^7 $CD62L^+$ cells was set as a starting material minimum before activation with anti-CD3/CD28 Transact reagent and lentiviral transduction. We found that this was readily achieved, with the umbilical cord blood units yielding: 1.33 x 10^8 (UCB1) and 0.96 x 10^8 (UCB2) $CD62L^+$ lymphocytes from donations of 1.2 x 10^9 and 8.2 x 10^8 MNCs, respectively **(Figure 2A, B and Table S3)**. Using MOIs of around 5, transduction efficiencies of 67% (UCB1) and 74% (UCB2) were achieved (**Figure 2C; Figure S1**).

Next, electroporation was performed 'off-device' using a Lonza LV for transient delivery of SpCas9 mRNA. Flow cytometry on day 7 found residual $TCR\alpha\beta^+$

(UCB1 34.6%; UCB2 35.4%) and $CD52^+$ (UCB1: 35.4%; UCB2 30.2%) (**Figure 2C; Figure S1**). 'On-device' prodigy expansion for 3 days was followed by automated bead-mediated depletion of residual $TCR\alpha\beta^+$ T cells with UCB1 exhibiting 0.2% and UCB2 0.3% $TCR\alpha\beta^+$ cells at the end of processing. Simultaneously, the CAR^+ fraction increased to >80% by the end of production as a result of coupling effects of editing and transduction in the TT52CAR19 configuration. Yields of 9.1×10^8 and 5.5×10^8 cells in total were achieved for UCB1 and UCB2, respectively. The product was cryopreserved in 1 ml aliquots of 1×10^7 (x 20 vials for each UCB1 and UCB2 batch) and 2×10^7 (x 10 vials for each UCB1 and UCB2 batch) total cells in individual vials and stored at <-130°C **(Table 1)**. Western blot and ELISA did not detect presence of Cas9 at the end of production **(Figure S2)**.

Phenotype & Molecular Characterisation of UCB-TT52CAR19

At the end of production >80% of cells were $CD45RA^+CD62L^+$ (**Figure S3)** with 85% - 92% CAR expression. Transduction was corroborated by proviral copy number by qPCR (UCB1 VCN: 2.7; UCB2 VCN: 4.0 copies/cell). On-target genome editing signatures of NHEJ were verified by quantification of insertions/deletions (indels) at TRAC (UCB1: 76%; UCB2: 59%) and CD52 (UCB1: 58%; UCB2: 51%) loci by ICE analysis of Sanger sequence traces (**Figure 3A; Figure S4A**). Targeted ddPCR quantification for NHEJ at these sites provided corroboration (TRAC: 65%, 47%; CD52: 73%, 38%) (**Figure 3B; Figure S4B**). Lentiviral integration was mapped by LM-PCR with the top ten most frequent sites presented in **Figure 4; Figure S5**.

End of production screening for aberrant DNA breaks

Karyotype analysis reported normal G-band analysis with no detection of chromosomal aberrations. Further investigations by FISH analysis found no evidence (within the limits of the probe set) of TRAD rearrangements in 197/200 cells (98.5%). Predictable translocation events were investigated (**Figure 5A; Figure S6A**) for four predicted recombinations (C1-C4) involving 14p (TRAC locus) and 1q (CD52 locus), and low frequency events (<1.0%) were quantified by ddPCR for each reaction, with 0.64% (UCB1) and 0.73% (UCB2) in total quantified over the four reactions.

Previously, Digenome-Seq analysis had informed design of screening for 'off-target' guide-dependent editing for the TT52CAR19 vector system. An abbreviated form of the screen was now applied at the six highest scoring

genomic sites (**Figure 5B; Figure S6B**). Targeted NGS found modification frequencies at these sites of <0.5% in both batches, whereas on-target NHEJ events were quantified as 65% and 51% at the TRAC locus and 73% and 17% at the CD52 locus for UCB1 and UCB2, respectively.

Functional studies of UCB-TT52CAR19 cells

The potency of each UCB-TT52CAR19 batch was assessed against ^{51}Cr labelled CD19$^+$ Daudi cells and CD19$^+$ or CD19$^-$ SupT1 cells (**Figure 6A; Figure S7A-C**). Specific lysis was demonstrated across a range of E:T ratios compared to untransduced (UnTD) cells (**P<0.01) with results comparable to TT52CAR19 products generated from adult PBL (**Figure 6B**). In addition, cytokine production was measured following a 1:1 co-culture with CD19$^+$ Daudi cells and CD19$^+$ or CD19$^-$ SupT1 cells (**Figure 6C; Figure S7D-F**) and secretion of cytokines IFN-γ, TNF-α, IL-4 and IL-2, compared to PBL derived TT52CAR19 cells (**Figure 6D**).

A chimeric human:murine xenograft model of B-cell malignancy was used to assess *in vivo* function of UCB-TT52CAR19 cells (**Figure 7A**). NSG mice were engrafted with 5 x 10^5 CD19$^+$eGFP$^+$Luciferase$^+$ Daudi cells and 5 x 10^6 UCB-TT52CAR19 effectors were infused 4 days later. Serial bioluminescence imaging over a 4-week period showed rapid disease progression in mice receiving UnTD cells, whereas mice treated with UCB-TT52CAR19 cells exhibited significantly reduced tumour signal and inhibition of disease throughout the monitoring period (UCB-UnTD GMP1 vs UCB-TT52CAR19 GMP1 (UCB1): P <0.0001; UCB-UnTD GMP2 vs UCB-TT52CAR19 GMP2 (UCB2): P <0.0001) (**Figure 7B, C; Figure S8**). Anti-leukaemic activity was similar to animals treated with PBL TT52CAR19 effector batches (UCB1 vs PBL P= 0.975; UCB2 vs PBL P = 0.986).

Discussion

Despite breakthroughs using autologous CAR T cells, there are notable hurdles to wider access to CAR therapies. Alternative “off-the-shelf" CAR T-cell banks suitable for multiple patients could ultimately reduce costs and avoid delays. Donor peripheral blood T cells have been successfully used to generate “universal” allogeneic CAR T cells. To overcome HLA mismatching, genome editing has been used to address the risk of GVHD by disrupting TCRαβ and

incorporating TCR$\alpha\beta$ depletion steps. Mitigations against host mediated rejection have included CD52 disruption to confer advantage in the presence of Alemtuzumab. Alternatively, direct disruption of HLA molecules, through editing of B_2M to prevent expression of HLA class I and class II by targeting transcription factors are under investigation and approaches to creating allogeneic universal banks have been reviewed recently [32, 33].

Umbilical cord donations may offer alternative sources of immune cells with potentially advantageous immunological properties. UCB derived NK cells have been of interest for their capacity to be used without HLA matching [22]. Trials have been underway for UCB NK cells transduced to express CAR19 and IL-15, to support antigen-driven expansion [21]. In a phase I clinical trial (NCT03056339) the first patients exhibited anti-leukaemic activity without severe toxicities [20]. Could cord blood T cells offer favourable expansion, persistence or longevity compared to adult PBLs? The importance of starting T-cell subsets for CAR-T manufacturing has been reported in pre-clinical and clinical studies [34, 35]. When peripheral blood selected naïve/stem cell memory (N/SCM) CD62L-positive CAR T cells were compared to unselected T cells, they appeared to provide better expansion and persistence and anti-leukaemic responses in chimeric mice [36]. One important caveat has been the interpretation of flow-based phenotyping using conventional memory/naïve panels which may not be straightforward after activation and transduction with CARs with different activation domains. Previous studies have included UCB units transduced with a retroviral vector incorporating CAR19 and an IL-12 transgene, which exhibited central memory phenotypes by the end of manufacture and expression of cytotoxic effector proteins Granzyme B and IFNγ [23]. Potent anti-leukaemic clearance in a preclinical mouse model of B-ALL was reported. In other work, cord blood units expressing anti-CD123 CAR T cells retained a less differentiated phenotype after activation and transduction, with anti-leukaemic activity *in vitro* and *in vivo* models [37]. We reasoned that CD62L could be an ideal selection target of cord T cells for manufacturing CAR T cells. In addition, a key hurdle in manufacturing from cord blood involves distinguishing T cells from other mononuclear cells. Cord blood is rich in nucleated red cells, causing difficulties in enumeration and analysis, and creating challenges for setting optimal culture and transduction conditions. Pre-selection using anti-CD62L magnetic bead enrichment allowed efficient automated enrichment of cord T cells ahead of activation. The process could be readily incorporated into a CliniMACS Prodigy matrix, and with compliant

reagents already available, included in established transduction and editing processes.

Overall, we found that CD62L^{+} cord CAR19 T cells exhibit expansion and anti-leukaemic activity *in vitro* and *in vivo*, comparable to control peripheral blood genome edited CAR19 T-cell products that have already been investigated in clinic [8]. Cord collection offers a further advantage in allowing ready access to a broad range of HLA haplotypes with tolerance for one or two antigen mismatches. Ultimately, the risk of host mediated rejection could be mitigated using batches of cells generated from donors homozygous for common HLA haplotypes. This could help avoid the need for intensive lymphodepletion currently applied to address barriers caused by HLA mismatches. It has been estimated that a large proportion of European populations could be partly, or fully HLA matched ,to 'off the shelf' cord blood banks derived from around 150 different donors [38]. Alternatively, as it is also now feasible to selectively remove mismatched HLA molecules from partially matched donations, a smaller pool of banked donations selectively retaining matched HLA molecules may prove sufficient [39].

In summary, UCB T cells can be isolated and enriched by CD62L selection and are amenable to machine-based gene modification, both using lentiviral vectors and by CRISPR-Cas9 editing. Potential therapeutic applications include 'off the shelf' CAR T therapies for ready access to products where autologous options are not available.

References

1. Maude SL, Laetsch TW, Buechner J, et al. Tisagenlecleucel in Children and Young Adults with B-Cell Lymphoblastic Leukemia. N Engl J Med. 2018;378(5):439-448.
2. Qayed M, McGuirk J, Myers G, et al. Leukapheresis guidance and best practices for optimal chimeric antigen receptor T-cell manufacturing. Cytotherapy. 2022;24(9):869-878.
3. Abecassis A, Roders N, Fayon M, et al. CAR-T cells derived from multiple myeloma patients at diagnosis have improved cytotoxic functions compared to those produced at relapse or following daratumumab treatment. EJHaem. 2022;3(3):970-974.
4. Brudno JN, Somerville RP, Shi V, et al. Allogeneic T Cells That Express an Anti-CD19 Chimeric Antigen Receptor Induce Remissions of B-Cell Malignancies That Progress After Allogeneic Hematopoietic Stem-Cell Transplantation Without Causing Graft-Versus-Host Disease. J Clin Oncol. 2016;34(10):1112-1121.
5. Zhang C, Wang XQ, Zhang RL, et al. Donor-derived CD19 CAR-T cell therapy of relapse of CD19-positive B-ALL post allotransplant. Leukemia. 2021;35(6):1563-1570.
6. Cruz CR, Micklethwaite KP, Savoldo B, et al. Infusion of donor-derived CD19-redirected virus-specific T cells for B-cell malignancies relapsed after allogeneic stem cell transplant: a phase 1 study. Blood. 2013;122(17):2965-2973.
7. Georgiadis C, Preece R, Nickolay L, et al. Long Terminal Repeat CRISPR-CAR-Coupled "Universal" T Cells Mediate Potent Anti-leukemic Effects. Mol Ther. 2018;26(5):1215-1227.
8. Ottaviano G, Georgiadis C, Gkazi S, et al. Phase 1 clinical trial of CRISPR-engineered CAR19 universal T cells for treatment of children with refractory B cell leukemia. Sci Transl Med. 2022;14(668):eabq3010.
9. Qasim W, Zhan H, Samarasinghe S, et al. Molecular remission of infant B-ALL after infusion of universal TALEN gene-edited CAR T cells. Sci Transl Med. 2017;9(374):eaaj2013.
10. Benjamin R, Graham C, Yallop D, et al. Genome-edited, donor-derived allogeneic anti-CD19 chimeric antigen receptor T cells in paediatric and adult B-cell acute lymphoblastic leukaemia: results of two phase 1 studies. Lancet. 2020;396(10266):1885-1894.
11. Kagoya Y, Guo T, Yeung B, et al. Genetic Ablation of HLA Class I, Class II, and the T-cell Receptor Enables Allogeneic T Cells to Be Used for Adoptive T-cell Therapy. Cancer Immunol Res. 2020;8(7):926-936.
12. Hu Y, Zhou Y, Zhang M, et al. Genetically modified CD7-targeting allogeneic CAR-T cell therapy with enhanced efficacy for relapsed/refractory CD7-positive hematological malignancies: a phase I clinical study. Cell Res. 2022;32(11):995-1007.
13. Webber BR, Lonetree CL, Kluesner MG, et al. Author Correction: Highly efficient multiplex human T cell engineering without double-strand breaks using Cas9 base editors. Nat Commun. 2019;10(1):5222.
14. Jo S, Das S, Williams A, et al. Endowing universal CAR T-cell with immune-evasive properties using TALEN-gene editing. Nat Commun. 2022;13(1):3453.
15. Iyer SP, Sica RA, Ho PJ, et al. The COBALT-LYM study of CTX130: a phase 1 dose escalation study of CD70-targeted allogeneic CRISPR-Cas9–engineered CAR T cells in patients with relapsed/refractory (R/R) T-cell malignancies. Hemasphere. 2022;6:163-164.
16. McGuirk J, Bachier CR, Bishop MR, et al. A phase 1 dose escalation and cohort expansion study of the safety and efficacy of allogeneic CRISPR-Cas9–engineered T cells (CTX110) in patients (Pts) with relapsed or refractory (R/R) B-cell malignancies (CARBON). J Clin Oncol. 2021;39(15_suppl):TPS7570.
17. Chiesa R, Georgiadis C, Syed F, et al. Base-Edited CAR7 T Cells for Relapsed T-Cell Acute Lymphoblastic Leukemia. N Engl J Med. 2023;389(10):899-910.
18. Mold J, Venkatasubrahmanyam S, Burt T, et al. Fetal and adult hematopoietic stem cells give rise to distinct T cell lineages in humans. Science. 2010;330(6011):1695-1699.

19. Chiesa R, Gilmour K, Qasim W, et al. Omission of in vivo T-cell depletion promotes rapid expansion of naïve CD4+ cord blood lymphocytes and restores adaptive immunity within 2 months after unrelated cord blood transplant. Br J Haematol. 2012;156(5):656-666.
20. Liu E, Marin D, Banerjee P, et al. Use of CAR-Transduced Natural Killer Cells in CD19-Positive Lymphoid Tumors. N Engl J Med. 2020;382(6):545-553.
21. Liu E, Tong Y, Dotti G, et al. Cord blood NK cells engineered to express IL-15 and a CD19-targeted CAR show long-term persistence and potent antitumor activity. Leukemia. 2018;32(2):520-531.
22. Shah N, Li L, McCarty J, et al. Phase I study of cord blood-derived natural killer cells combined with autologous stem cell transplantation in multiple myeloma. Br J Haematol. 2017;177(3):457-466.
23. Pegram H, Purdon T, van Leeuwen D, et al. IL-12-secreting CD19-targeted cord blood-derived T cells for the immunotherapy of B-cell acute lymphoblastic leukemia. Leukemia. 2015;29(2):415-422.
24. Riddell S, Sommermeyer D, Berger C, et al. Adoptive therapy with chimeric antigen receptor-modified T cells of defined subset composition. Cancer J. 2014;20(2):141-144.
25. Kwoczek J, Riese S, Tischer S, et al. Cord blood-derived T cells allow the generation of a more naïve tumor-reactive cytotoxic T-cell phenotype. Transfusion. 2018;58(1):88-99.
26. Sallusto F, Geginat J, Lanzavecchia A. Central memory and effector memory T cell subsets: function, generation, and maintenance. Annu rev Immunol. 2004;22:745-763.
27. Kellner J, Yvon E, Parmar S. Ex vivo generation of umbilical cord blood T regulatory cells expressing the homing markers CD62L and cutaneous lymphocyte antigen. Oncotarget. 2018;9(72):33694-33701.
28. Kim D, Bae S, Park J, et al. Digenome-seq: genome-wide profiling of CRISPR-Cas9 off-target effects in human cells. Nat Methods. 2015;12(3):237-243.
29. Georgiadis C, Rasaiyaah J, Gkazi S, et al. Base-edited CAR T cells for combinational therapy against T cell malignancies. Leukemia. 2021;35(12):3466-3481.
30. Mock U, Hauber I, Fehse B. Digital PCR to assess gene-editing frequencies (GEF-dPCR) mediated by designer nucleases. Nat Protoc. 2016;11(3):598-615.
31. Mock U, Machowicz R, Hauber I, et al. mRNA transfection of a novel TAL effector nuclease (TALEN) facilitates efficient knockout of HIV co-receptor CCR5. Nucleic Acids Res. 2015;43(11):5560-5571.
32. Qasim W. Genome-edited allogeneic donor "universal" chimeric antigen receptor T cells. Blood. 2023;141(8):835-845.
33. Martin KE, Hammer Q, Perica K, Sadelain M, Malmberg K-J. Engineering immune-evasive allogeneic cellular immunotherapies. Nat Rev Immunol. 2024 Apr 24. [Epub ahead of print]
34. Fraietta JA, Lacey SF, Orlando EJ, et al. Determinants of response and resistance to CD19 chimeric antigen receptor (CAR) T cell therapy of chronic lymphocytic leukemia. Nat Med. 2018;24(5):563-571.
35. Xu Y, Zhang M, Ramos C, et al. Closely related T-memory stem cells correlate with in vivo expansion of CAR.CD19-T cells and are preserved by IL-7 and IL-15. Blood. 2014;123(24):3750-3759.
36. Arcangeli S, Bove C, Mezzanotte C, et al. CAR T cell manufacturing from naive/stem memory T lymphocytes enhances antitumor responses while curtailing cytokine release syndrome. The J Clin Invest. 2022;132(12):e150807.
37. Caël B, Galaine J, Bardey I, et al. Umbilical Cord Blood as a Source of Less Differentiated T Cells to Produce CD123 CAR-T Cells. Cancers (Basel). 2022;14(13):3168.
38. Taylor CJ, Peacock S, Chaudhry AN, Bradley JA, Bolton EM. Generating an iPSC bank for HLA-matched tissue transplantation based on known donor and recipient HLA types. Cell Stem Cell. 2012;11(2):147-152.
39. Xu H, Wang B, Ono M, et al. Targeted Disruption of HLA Genes via CRISPR-Cas9 Generates iPSCs with Enhanced Immune Compatibility. Cell Stem Cell. 2019;24(4):566-578.e7.

Tables:

Table 1. UCB-TT52CAR19 GMP1 and GMP2 end of manufacture batch specifications.

	UCB-TT52CAR19-GMP1 (UCB1)	UCB-TT52CAR19-GMP2 (UCB2)
Viability (7AAD[1])	96.2%	99.8%
CAR19 Transduction Efficiency	88.7%	82.8%
Purification	0.2% CD45+TCRαβ+ cells	0.3% CD45+TCRαβ+ cells
Sterility (BACTEC[2])	No Growth	No Growth
Sterility (Gram stain)	No Organisms Seen	No Organisms Seen
Mycoplasma	None Detected	None Detected
Endotoxin	<1.0 EU/ml	<1.0 EU/ml
Yield	906×10^6	546×10^6

[1] 7-Aminoactinomycin D (7AAD) used as fluorescent probe of non-viable cell exclusion

[2] BACTEC blood culture media for detection of aerobes, anaerobes, yeast, fungi and mycobacteria

Figure legends

Figure 1. Schematic timeline for GMP manufacturing of TT52CAR19 cell banks from Umbilical Cord Blood (UCB) starting material. Fresh UCB units were enriched for lymphocytes by $CD62L^+$ magnetic bead positive selection and activated on day 0 (D0). T cells were transduced 24hrs later (D1) with TT52CAR19 vector and electroporated on day 4 (D4) with SpCas9 mRNA. On day 11 (D11), cells underwent automated TCRαβ T-cell depletion. After this step the final cell product was harvested and cryopreserved in therapeutic doses. Steps itemised below the timeline were performed on a Miltenyi Prodigy and are shown as 'On-device', with the remaining items (above the timeline) undertaken off-device.

Figure 2. Whole UCB CD62L selection using the CliniMACS Prodigy and TT52CAR19 batch manufacture. A. UCB cells pre and post $CD62L^+$ selection using the CliniMACS Prodigy demonstrates enrichment of $CD3^+$ T cells. **B.** Cord blood cells from UCB donors (n=4) were analysed by Sysmex pre and post CD62L selection using the CliniMACS Prodigy. **C.** Flow cytometric T-cell transduction and knockout analysis of UCB-TT52CAR19 GMP1 (UCB1) cell bank. UCB-TT52CAR19 cells were stained before and after up to two rounds of magnetic TCRαβ depletion alongside untransduced (UnTD) cells or non-edited UCB-TT52CAR19 TCR^+ cells. Transduction efficiency was measured by quantifying transgene expression using F(ab')2, and CRISPR-Cas9 mediated protein knockout was determined through staining for TCRαβ and CD52.

Figure 3. Molecular characterisation of on-target CRISPR-Cas9 mediated cleavage. (A) ICE analysis of Sanger sequence traces identified indels as signatures of NHEJ at the TRAC locus and at the CD52 target site. **(B)** Quantification of indels by ddPCR at both the TRAC and CD52 sites using separate probes, one specific to the predicted NHEJ region ($NHEJ^+$) and a second outside the NHEJ region ($NHEJ^-$).

Figure 4. Integration site analysis. Ligation-mediated PCR (LMPCR) detection and quantification of vector integration sites (IS) where the top 10 most frequent sites comprised <0.1% of integrants.

Figure 5. Detection for translocation and off-target CRISPR-Cas9 mediated cleavage events (A) Droplet Digital PCR (ddPCR) was used for the detection and quantification of possible translocations after 'on-target' DNA scission. Four predicted recombination events (C1-C4) are presented in the schematic with TRAC (Chr14q) (green), CD52 (Chr1p) (red) and SpCas9 cleavage site (red line). Right panel colours (yellow, green, magenta, blue) discriminate four possible translocations. Left panel shows low frequency translocation events (blue dots) C1-C4 arising between the edited TRAC and CD52 loci. Cumulative events for all four possible events were <1%. **(B)** Circos plot with verification of quantification using targeted NGS across six highest scoring predicted off-target sites. TRAC-01 (solid red line marking locus in outer yellow circle), CD52-01 (solid red line marking inner yellow circle) and at predicted off-target sites TRAC-02-TRAC-07 (red arrows marking outer yellow circle) and CD52-02-CD52-07 (red arrows marking inner yellow circle). Table shows that negligible off-target events were detected for both the TRAC and CD52 guides.

Figure 6. *In vitro* killing potential and cytokine production of UCB-TT52CAR19 cells against $CD19^+$ targets. *In vitro* cytotoxicity of UCB-TT52CAR19 GMP1 (UCB1) cell bank compared to respective UCB-TT52CAR19 transduced but not edited (UCB-TT52CAR19 TCR^+) or non-transduced (UnTD) controls **(A)** or PBL-TT52CAR19 effectors and respective controls **(B)** when measured by ^{51}Cr chromium release of labelled $CD19^+$ Daudi cells following four hours of co-culture at incremental effector (E) – target (T) ratio. Cell co-cultures ranged from $1 \times 10^5 : 5 \times 10^4$ (at E:T of 20:1) to $8 \times 10^2 : 5 \times 10^4$ (at E:T of 0.16:1). Effector responses were considered successful if ≥50% lysis was detected compared to UnTD controls at E:T cell ratios between 1.25:1 and 5:1. Error bars SEM, n=3 replicate/wells. *P < 0.05, **P < 0.01, ***P < 0.001 by t-test. In vitro target specific cytokine secretion of UCB-TT52CAR19 GMP1 cell bank (UCB1), and respective UCB-TT52CAR19 TCR^+ or non-transduced (UnTD) controls after co-culture with $CD19^+$ Daudi cells overnight **(C)**. Cytokine release also quantified for PBL-TT52CAR19 effectors and respective PBL-TT52CAR19 TCR^+ and UnTD control at 1:1 E:T (1.25×10^5 of each effector and target cells) co-cultures with $CD19^+$ Daudi cells **(D)** The presence of cytokines in the co-culture supernatant was measured by cytokine bead array and levels >50 pg/ml were considered positive responses. Significance was calculated between UCB-TT52CAR19 GMP1 (UCB1) or PBL-TT52CAR19 banks and respective UnTD controls. *P < 0.05 by t-test. Error bars represent SEM, n=3 replicates.

Figure 7. *In vivo* tumour clearance in human:murine xenograft model of $CD19^+$ disease.

Timeline of *in vivo* human:murine xenograft modelling indicating target and effector intravenous injection days and bioluminescent imaging (BLI) timepoints **(A)**. Serial measurement of bioluminescence of Daudi $CD19^+$ B-cell disease in immunodeficient mice NOD/SCID/γc (NSG) mice (n=12) infused with 5×10^5 GFP/luciferase expressing Daudi $CD19^+$ B cells were treated on day 4 with 5×10^6 of either umbilical cord blood (UCB) UCB-TT52CAR19 GMP1 (UCB1) (n=5) or peripheral blood lymphocyte (PBL) PBL-TT52CAR19 (n=4) and were monitored over a 4 week period **(B, C)** Non-transduced (UnTD) (n=4) T cells were used as controls. Error bars represent SEM. Significance compared by area under the curve using one-way ANOVA (F-value 35.86) with Tukey multiple comparison post-hoc; not significant (ns) P ≥ 0.05; ****P < 0.0001.

Figure 1

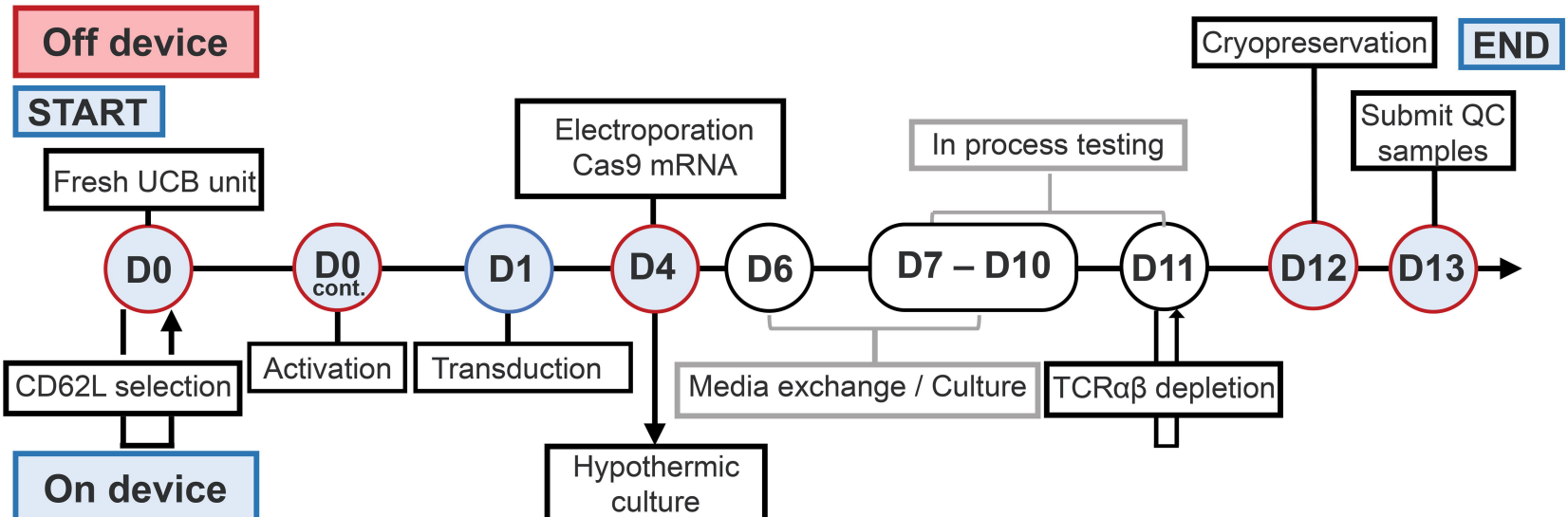
Off device
START
Fresh UCB unit
D0
D0 cont.
D1
D4
D6
D7 – D10
D11
D12
D13
Electroporation Cas9 mRNA
In process testing
Cryopreservation
END
Submit QC samples
CD62L selection
Activation
Transduction
Media exchange / Culture
TCRαβ depletion
On device
Hypothermic culture

Figure 2

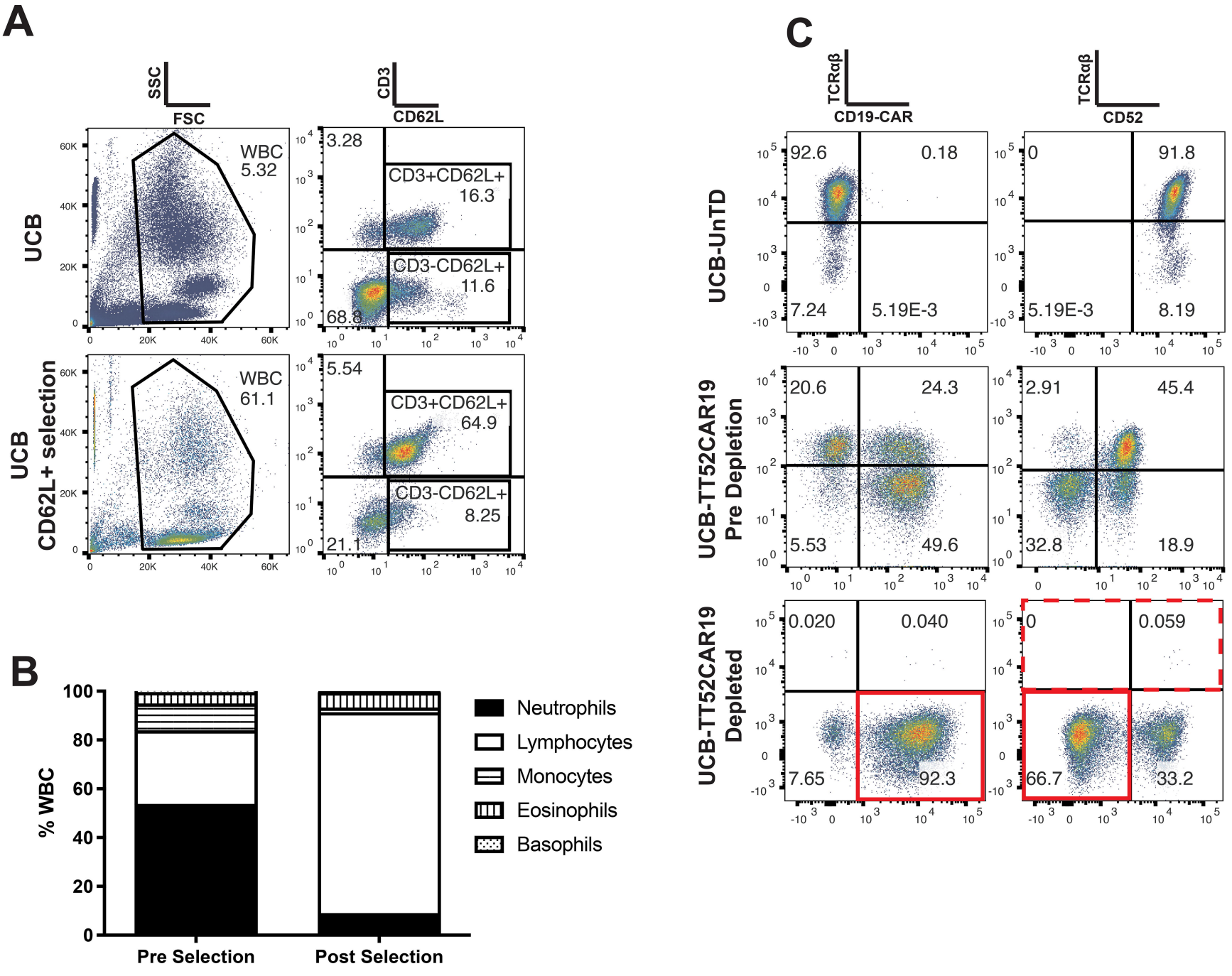
A
SSC
FSC
CD3
CD62L
UCB
WBC
5.32
3.28
CD3+CD62L+
16.3
CD3-CD62L+
11.6
68.8
UCB
CD62L+ selection
WBC
61.1
5.54
CD3+CD62L+
64.9
CD3-CD62L+
8.25
21.1
B
% WBC
Pre Selection
Post Selection
Neutrophils
Lymphocytes
Monocytes
Eosinophils
Basophils
C
TCRαβ
CD19-CAR
CD52
UCB-UnTD
92.6
0.18
7.24
5.19E-3
0
91.8
5.19E-3
8.19
UCB-TT52CAR19
Pre Depletion
20.6
24.3
5.53
49.6
2.91
45.4
32.8
18.9
UCB-TT52CAR19
Depleted
0.020
0.040
7.65
92.3
0
0.059
66.7
33.2

Figure 3

A

TRAC Guide Target	PAM	r^2	KO-score
TCTCTCAGCTGGTACACGGC	AGG	0.9	76

INDEL	Contribution	Sequence
-2	18.3%	AGATATCCAGAACCCTGACCCTGCC--GTACCAGCTGAGAGACT
0	14.9%	AGATATCCAGAACCCTGACCCTGCCGTGTACCAGCTGAGAGACT
+1	10.1%	AGATATCCAGAACCCTGACCCTGCCNGTGTACCAGCTGAGAGAC
-1	6.9%	AGATATCCAGAACCCTGACCCTGCC-TGTACCAGCTGAGAGACT
-11	6.1%	AGATATCCAGAACCCTGAC------CCAGCTGAGAGACT
-2	5.4%	AGATATCCAGAACCCTGACCCTG--GTGTACCAGCTGAGAGACT
-7	3.6%	AGATATCCAGAACCCTGA-------GTGTACCAGCTGAGAGACT
-2	3.5%	AGATATCCAGAACCCTGACCCTGC-TGTACCAGCTGAGAGACT
-12	2.7%	AGATATCCAGAACCCTGACCCT---CTGAGAGACT
-7	2.6%	AGATATCCAGAACCCTGACCCTG--CCAGCTGAGAGACT
-3	2.6%	AGATATCCAGAACCCTGACCCTG--TACCAGCTGAGAGACT
-24	1.3%	AGATATCCAGAAC----------AGAGACT
-20	1.2%	AGATATCCAGAACC----------CTGAGAGACT
-5	1.2%	AGATATCCAGAACCCTGACCCTG--TACCAGCTGAGAGACT

CD52 Guide Target	PAM	r^2	KO-score
TACCATAACCAGGAGGCTGA	TGG	0.93	58

INDEL	Contribution	Sequence
0	35.2%	CTTACCTGTACCATAACCAGGAGGCTGATGGTGAGTAGGAG
+1	28.3%	CTTACCTGTACCATAACCAGGAGGCNTGATGGTGAGTAGGA
-1	10.3%	CTTACCTGTACCATAACCAGGAGG-TGATGGTGGATAGGAG
-18	6.5%	CTTACCTGTACCATAACCAG-----------GAG
-7	3.6%	CTTACCTGTACCATAACCAGGAG--GTGAGTAGGAG
-12	1.9%	CTTACCTGTACCATAACCAG-----GAGTAGGAG
-18	1.8%	CTTACCTGTA----------TGGTGAGTAGGAG
+2	1.3%	CTTACCTGTACCATAACCAGGAGGCNNTGATGGTGAGTAGG
-4	1%	CTTACCTGTACCATAACCAGGA---GATGGTGAGTAGGAG
-18	1%	CTTACCTGTACCATAAC---------TAGGAG

B

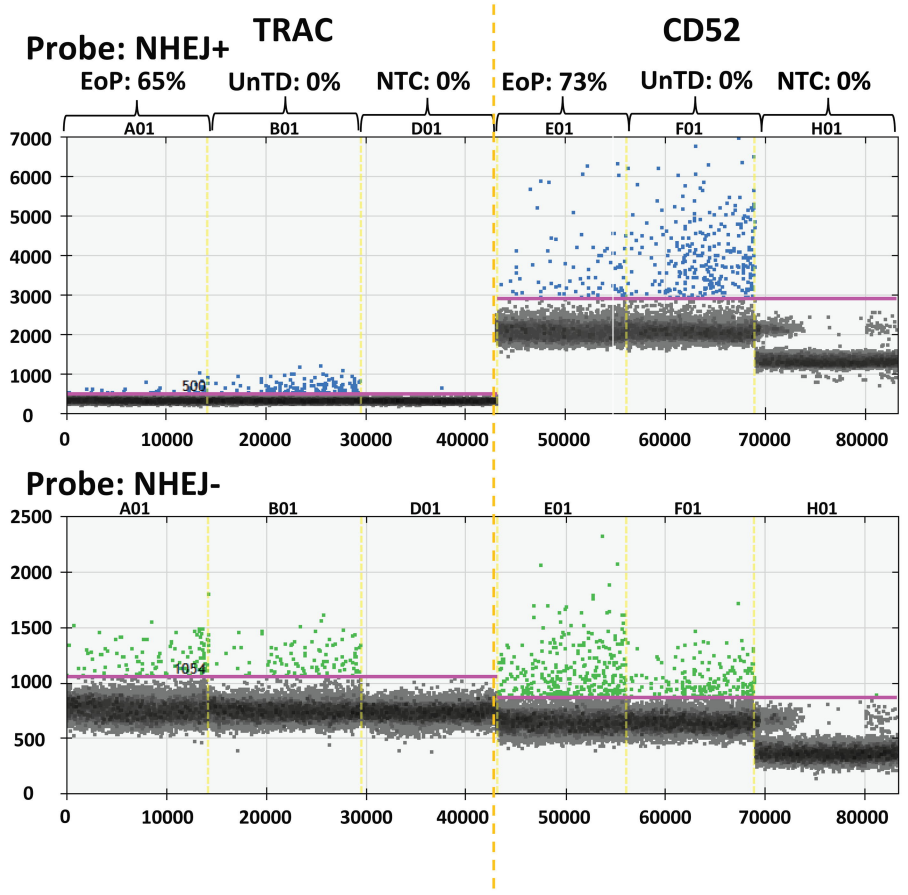

Figure 4

Rank	Gene Name	Frequency [%]	Location
Top1	EIF5A	0.069	17-7304911
Top2	SPIN4	0.061	X-63353021
Top3	DNAJC7	0.06	17+41988746
Top4	ATP11B	0.058	3+182905619
Top5	LRMP	0.056	12+25058347
Top6	RNASET2	0.055	6-166958978
Top7	APOO	0.055	X-23850789
Top8	FAM222B	0.054	17+28801017
Top9	MLXIP	0.054	12-122135898
Top10	CEP97	0.053	3-101760227
#All Other mapp. IS	14106	99.425	

Eq Count 10 Strongest	564
Count all other mapp .IS	97465
Total Seq Counts Used	98029

Figure 5

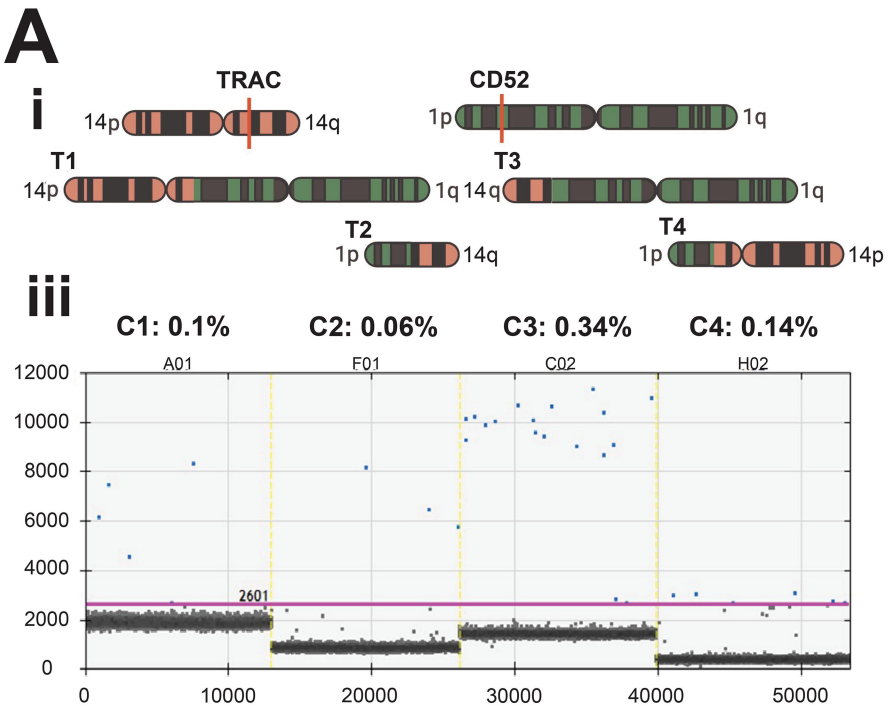

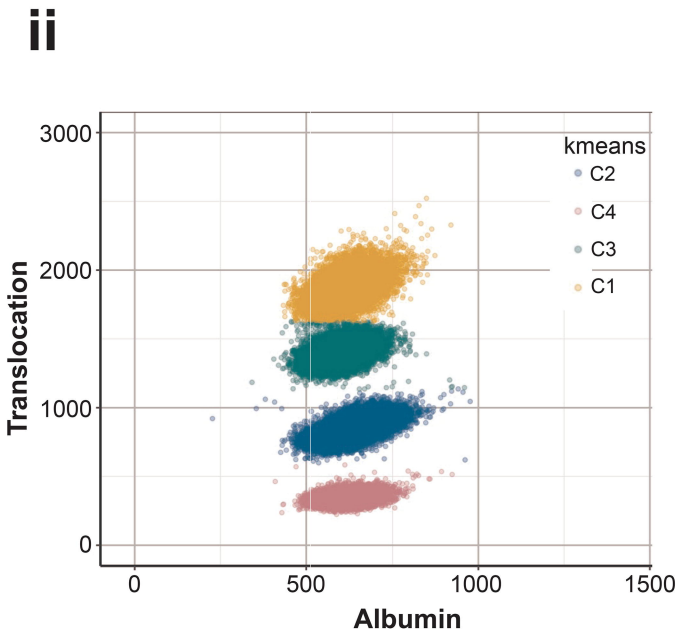

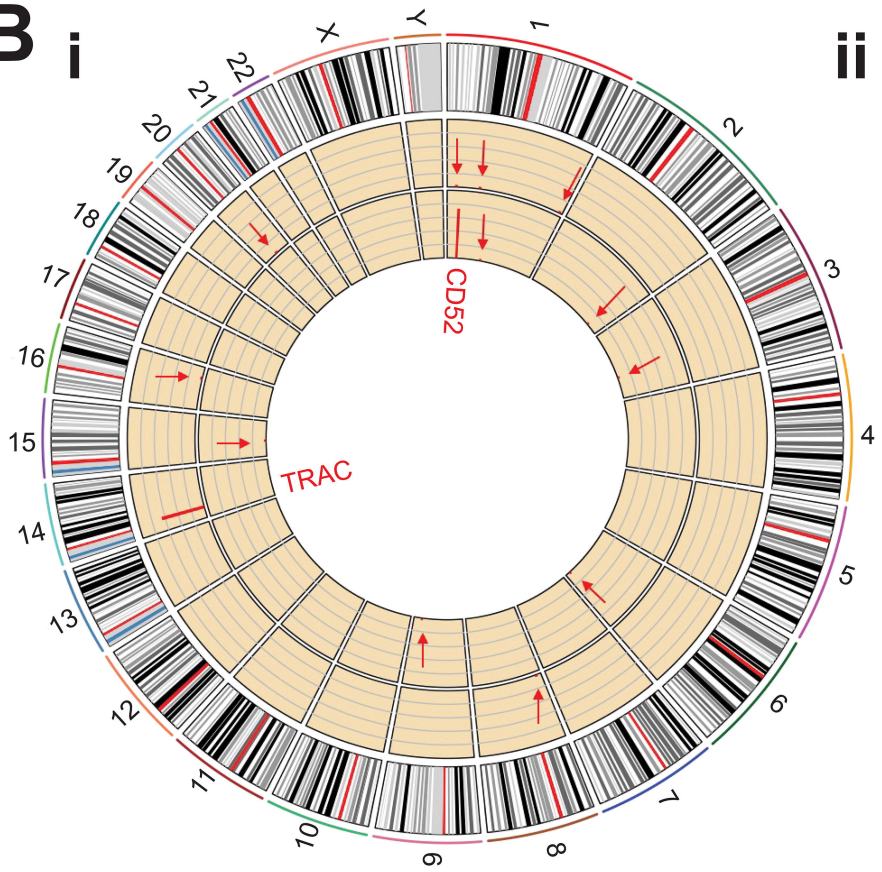

ii

TRAC

Index	Chromosome	ChromStart	ChromEnd	Mutant Frequency
TRAC-01	chr14	23016465	23016487	65
TRAC-02	chr8	10627242	10627255	0.03
TRAC-03	chr1	68621798	68621815	0.03
TRAC-04	chr1	19612375	19612394	0.05
TRAC-05	chr1	242872248	242872256	0.15
TRAC-06	chr20	31622178	31622197	0.06
TRAC-07	chr16	66528021	66528030	0.03

CD52

Index	Chromosome	ChromStart	ChromEnd	Mutant Frequency
CD52-01	chr1	26644530	26644550	73
CD52-02	chr9	118431460	118431490	0.04
CD52-03	chr15	45497075	45497095	0.02
CD52-04	chr1	95875500	95875515	0.03
CD52-05	chr2	207739015	207739040	0.02
CD52-06	chr3	135905235	135905255	0.04
CD52-07	chr6	156954690	156954710	0.03

Figure 6

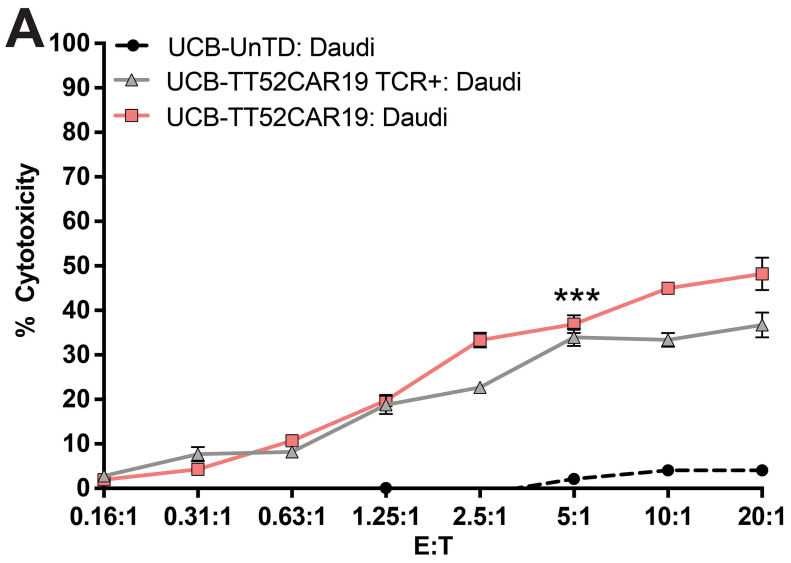
A
UCB-UnTD: Daudi
UCB-TT52CAR19 TCR+: Daudi
UCB-TT52CAR19: Daudi
% Cytotoxicity
E:T
0.16:1
0.31:1
0.63:1
1.25:1
2.5:1
5:1
10:1
20:1
***

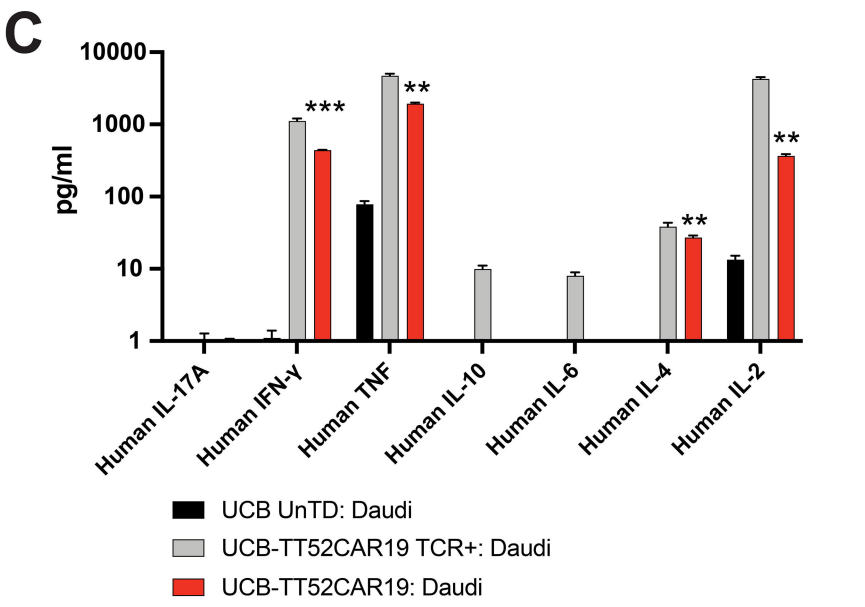
C
pg/ml
Human IL-17A
Human IFN-γ
Human TNF
Human IL-10
Human IL-6
Human IL-4
Human IL-2
UCB UnTD: Daudi
UCB-TT52CAR19 TCR+: Daudi
UCB-TT52CAR19: Daudi

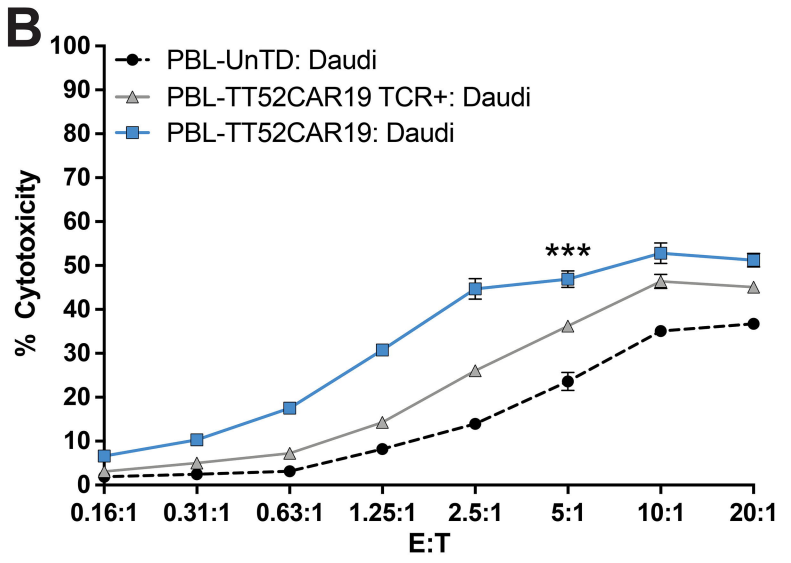
B
PBL-UnTD: Daudi
PBL-TT52CAR19 TCR+: Daudi
PBL-TT52CAR19: Daudi
% Cytotoxicity
E:T
0.16:1
0.31:1
0.63:1
1.25:1
2.5:1
5:1
10:1
20:1
***

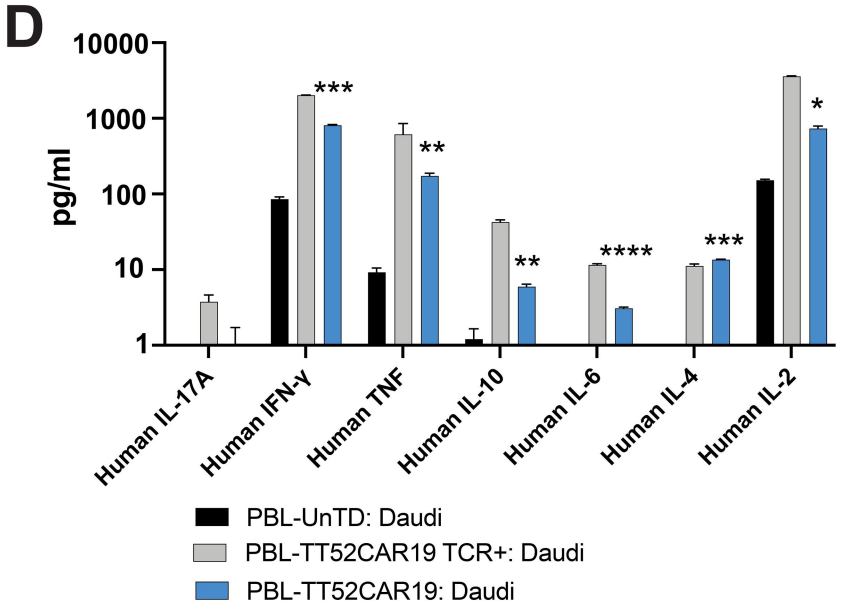
D
pg/ml
Human IL-17A
Human IFN-γ
Human TNF
Human IL-10
Human IL-6
Human IL-4
Human IL-2
PBL-UnTD: Daudi
PBL-TT52CAR19 TCR+: Daudi
PBL-TT52CAR19: Daudi

Figure 7

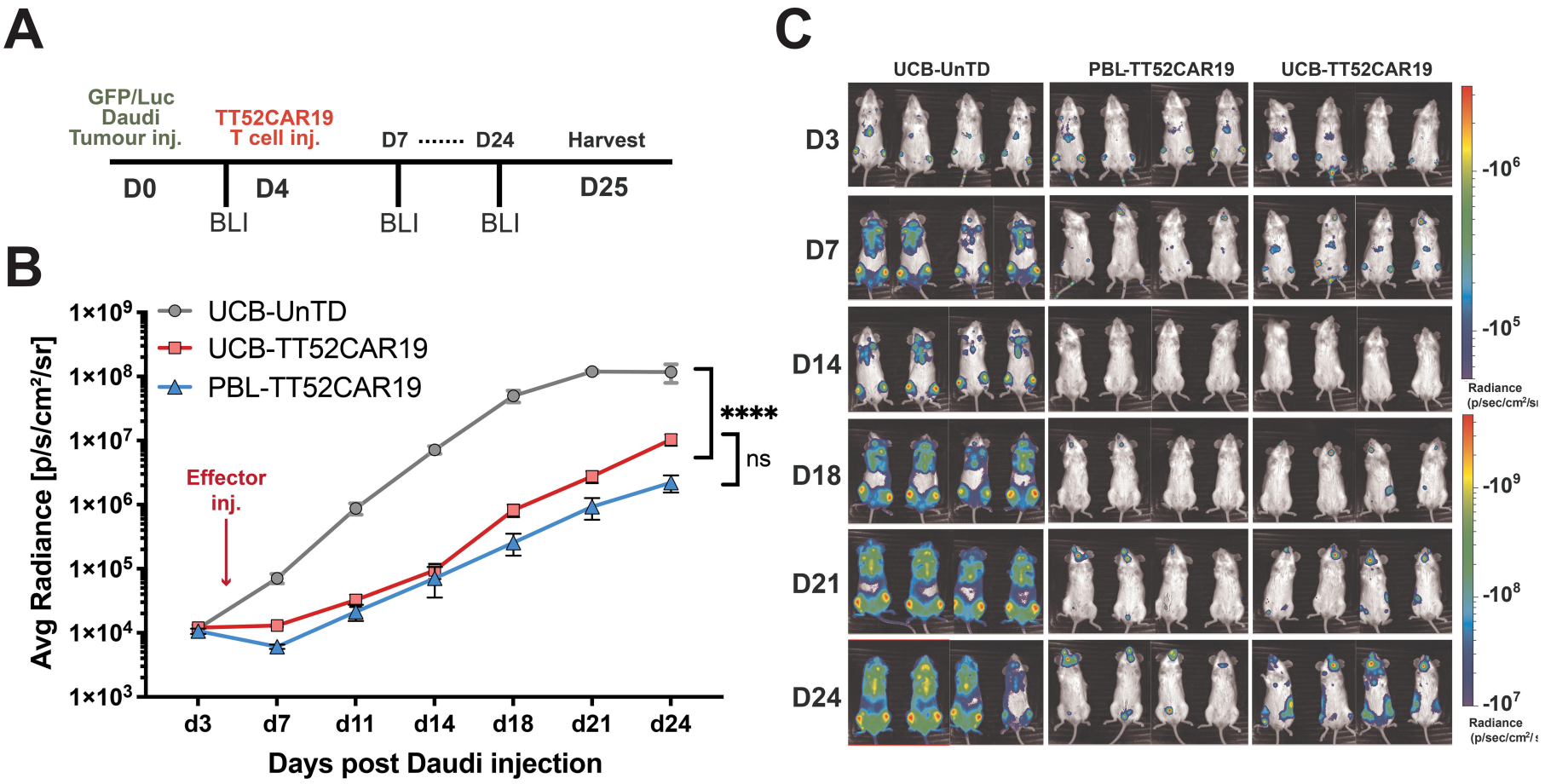
A
GFP/Luc
Daudi
Tumour inj.
TT52CAR19
T cell inj.
D7 ····· D24
Harvest
D0
D4
D25
BLI
BLI
BLI
B
UCB-UnTD
UCB-TT52CAR19
PBL-TT52CAR19
Avg Radiance [p/s/cm²/sr]
1×10⁹
1×10⁸
1×10⁷
1×10⁶
1×10⁵
1×10⁴
1×10³
Effector
inj.
****
ns
d3
d7
d11
d14
d18
d21
d24
Days post Daudi injection
C
UCB-UnTD
PBL-TT52CAR19
UCB-TT52CAR19
D3
D7
D14
D18
D21
D24
-10⁶
-10⁵
Radiance
(p/sec/cm²/s
-10⁹
-10⁸
-10⁷
Radiance
(p/sec/cm²/

Umbilical cord blood T cells can be isolated and enriched by CD62L selection for use in 'off the shelf' chimeric antigen receptor T-cell therapies to widen transplant options

Christos Georgiadis[1], Lauren Nickolay[1], Farhatullah Syed[1], Hong Zhan[1], Soragia Athina Gkazi[1], Annie Etuk[1], Ulrike Abramowski-Mock[1], Roland Preece[1], Piotr Cuber[1], Stuart Adams[2], Giorgio Ottaviano[1] and Waseem Qasim[1,2]

[1] UCL Great Ormond Street Institute of Child Health, WC1N 1DZ, London, UK

[2] Great Ormond Street Hospital for Children NHS Trust, WC1N 3JH, London, UK

Supplementary Materials and Methods

Determination of vector copy number (VCN)

CAR19 transgene in transduced cells was assessed by VCN in genomic DNA at end of manufacture of UCB-TT52CAR19 at GOSH NHS Trust. Vector copies were determined by qPCR or droplet digital PCR (ddPCR) targeting HIV-psi or human albumin sequences **(Table S1)**.

Karyotype and Fluorescence in Situ Hybridization (FISH)

UCB-TT52CAR19 cells were cultured with Colcemid overnight in order to arrest cells in metaphase. Karyotype using Giemsa-Banding (G-Banding) and fluorescence in situ hybridization (FISH) analysis was performed at GOSH NHS trust; the latter used a dual colour, break-apart FISH probe (Cytocell TCRAD LPH 047-S; 14q11, red/green fusion) to interrogate interphase nuclei.

Quantification of on- and off-target editing effects and translocations (continued)

On-target and off-target sites informed by previous Digenome-seq studies were captured using Phusion polymerase (New England BioLabs), and the products amplified using TruSeq HT Dual Index primers **(Table S1)**. Libraries were then subjected to paired-end Next Generation Sequencing (NGS) using MiniSeq (Illumina) as previously described. Demultiplexed fastq files were uploaded to Galaxy for quality checks, trimming and alignment. Non-homologous end joining (NHEJ) signatures were analysed using Pindel and figures were created in R.

Vector integration site analysis

Lentiviral integration sites (IS) were mapped by Genwerks (Protagene, Germany) using Shearing Extension Primer Tag Selection Ligation-Mediated PCR (S-EPTS/LM PCR) as previously described [1] and the top 10 most frequent loci tabulated.

Cytokine Bead Array

Cytokine release was quantified after overnight co-culture of UCB-TT52CAR19 GMP1 (UCB1) and GMP2 (UCB2) or PBL derived batches alongside TT52CAR19 TCR+ or UnTD control cells with CD19+Daudi and $CD19^{+}$ or $CD19^{-}$ SupT1 cells at a 1:1 ratio using a TH1/TH2/TH17 human bead array kit (Becton Dickinson Biosciences).

References

1. Ottaviano G, Georgiadis C, Gkazi S, et al. Phase 1 clinical trial of CRISPR-engineered CAR19 universal T cells for treatment of children with refractory B cell leukemia. Science translational medicine. 2022;14(668):

Supplementary Figure S1.

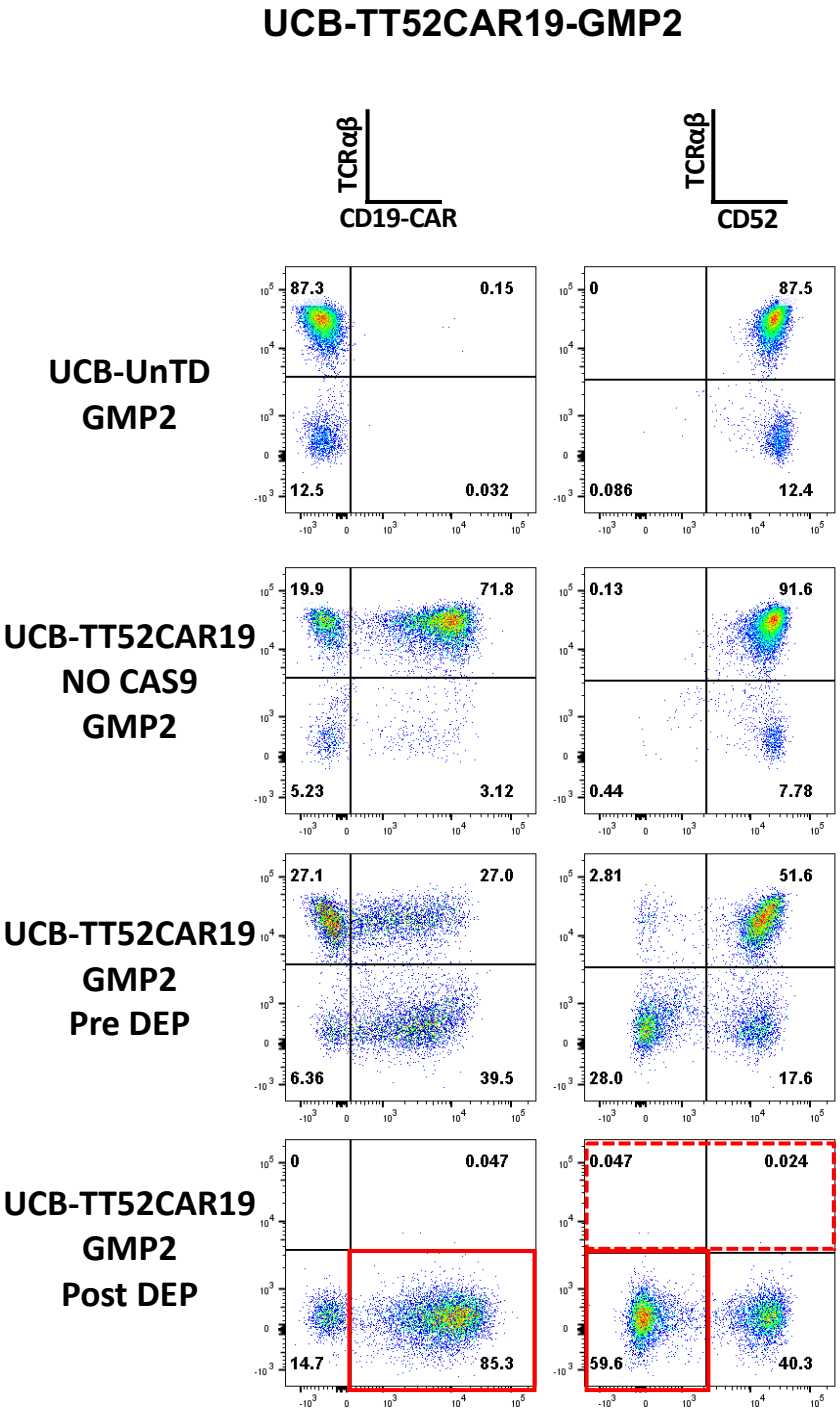

Supplementary Figure S1. CAR19 and TCRαβ phenotyping of UCB-TT52CAR19 GMP2 bank throughout manufacture. Flow cytometric T cell transduction and knockout analysis of UCB-TT52CAR19 GMP2 (UCB2) cell bank. UCB-TT52CAR19 cells were stained pre and post magnetic TCRαβ depletion alongside untransduced (UnTD) cells or non-edited UCB-TT52CAR19 TCR+ cells. Transduction efficiency was measured by quantifying transgene expression using F(ab')2, and CRISPR/Cas9 mediated protein knockout was determined through staining for TCRαβ and CD52.

Supplementary Figure S2.

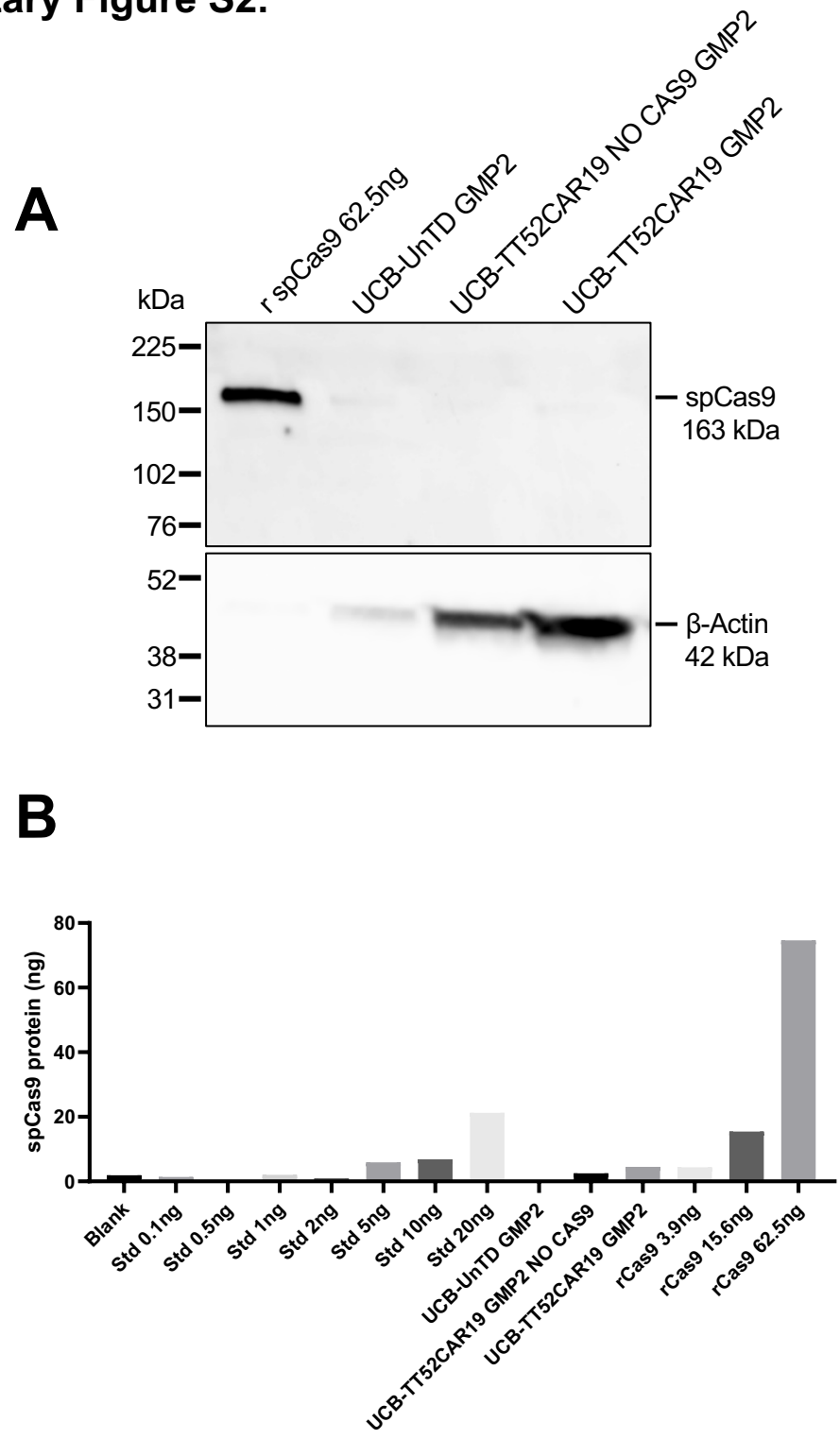

Supplementary Figure S2. End of production verification of absence of residual SpCas9 protein. (A) Whole cell lysate (20µg) from end of production UCB-TT52CAR19 GMP2 (UCB2) cells (lane 4), untransduced (UnTD) (lane 2) or non-edited UCB-TT52CAR19 NO CAS9 GMP2 (lane 3) was subjected to western blot SDS-PAGE and stained with a rabbit polyclonal anti-CRISPR-Cas9 antibody (ab191468, abcam, Cambridge, UK). Absence of specific bands at 163 kDa confirmed the absence of residual SpCas9 protein. Recombinant SpCas9 (rCas9) protein (62.5ng) (lane 1) was used as a positive control. **(B)** Whole cell lysate (5µg) from end of production UCB-TT52CAR19 GMP2 (UCB2) cells, untransduced (UnTD) or non-edited UCB-TT52CAR19 NO CAS9 GMP2 was analysed by EpiQuik CRISPR/Cas9 Assay ELISA Kit (Colorimetric) (EpigenTek, US) against manufacturer's standards (Std) and recombinant SpCas9 (rCas9) protein positive controls. SpCas9 protein levels in end of production UCB samples were comparable to blank control.

Supplementary Figure S3.

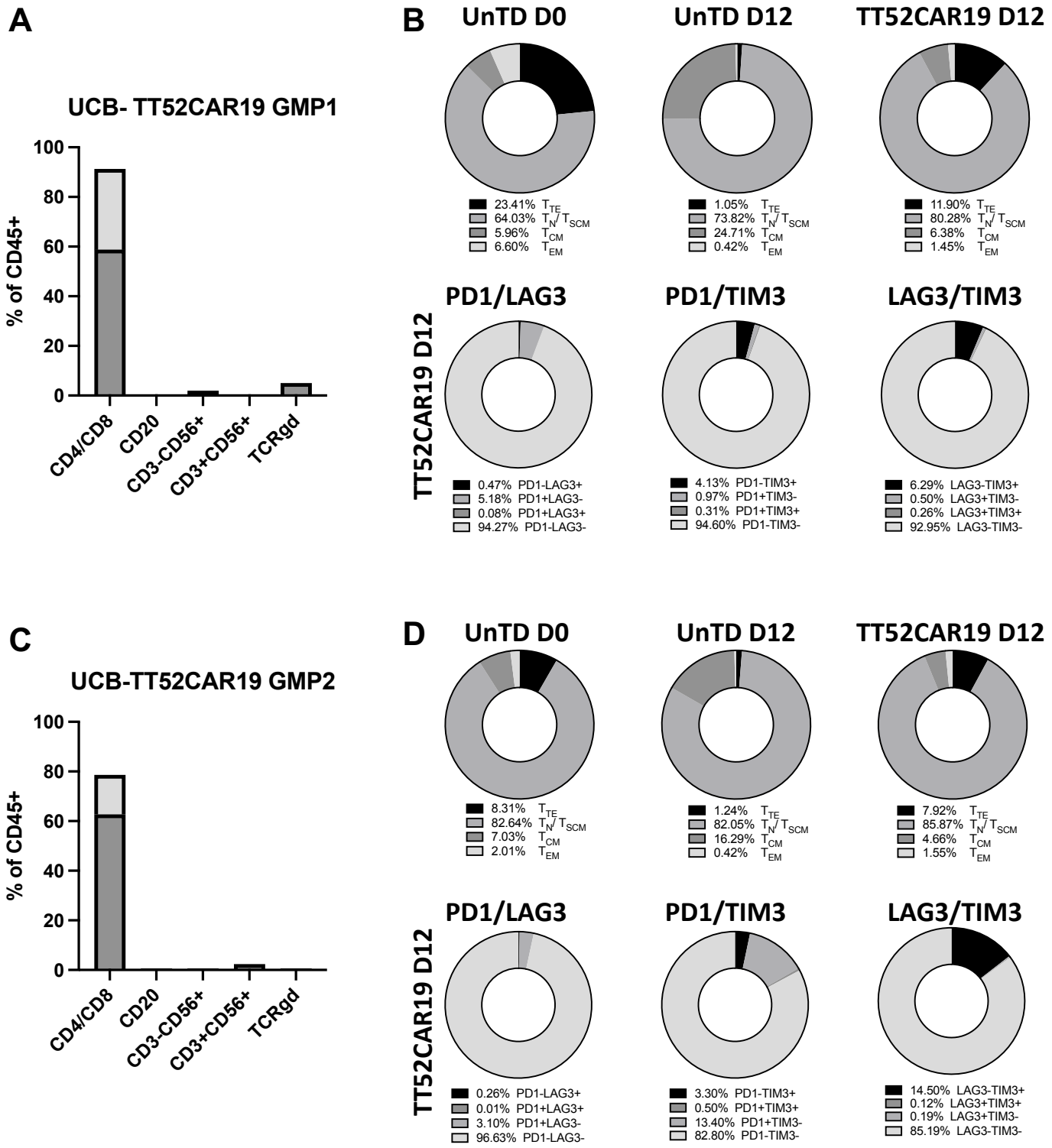

Supplementary Figure S3. Memory phenotype of end of production UCB-TT52CAR19 GMP batches. End of production UCB-TT52CAR19 cells, untransduced (UnTD) cells from day 0 (D0) and day 12 (D12) or UCB-TT52CAR19 cells from GMP batches GMP1 (UCB1) (top) or GMP2 (UCB2) (bottom) were phenotyped by flow cytometry. **(A, C)** Lymphocyte subset distribution of the two cell banks: T cells represented by combined CD4+ cells (dark grey) and $CD8^+$ (light grey); B cells expressing $CD20^+$; NK and T/NK cells ($CD3^-CD56^+$ and $CD3^+CD56^+$, respectively); TCRγδ T cells; **(B top, D top)** T cell subsets exhibited surface markers $CD45RA^+CD62L^+$ attributed to naïve T cells (TN) and memory stem cell T cells (TSCM). Remaining subsets represented differentiated $CD45RA^-CD62L^+$ central memory (TCM), $CD45RA^+CD62L^-$ terminal effectors (TTE) and $CD45RA^-CD62L^-$ effector memory (TEM) T cells; **(B bottom, D bottom)** Profiling of activation/exhaustion of the three cell banks was investigated using three co-inhibitory markers (PD-1, TIM3, LAG3).

Supplementary Figure S4.

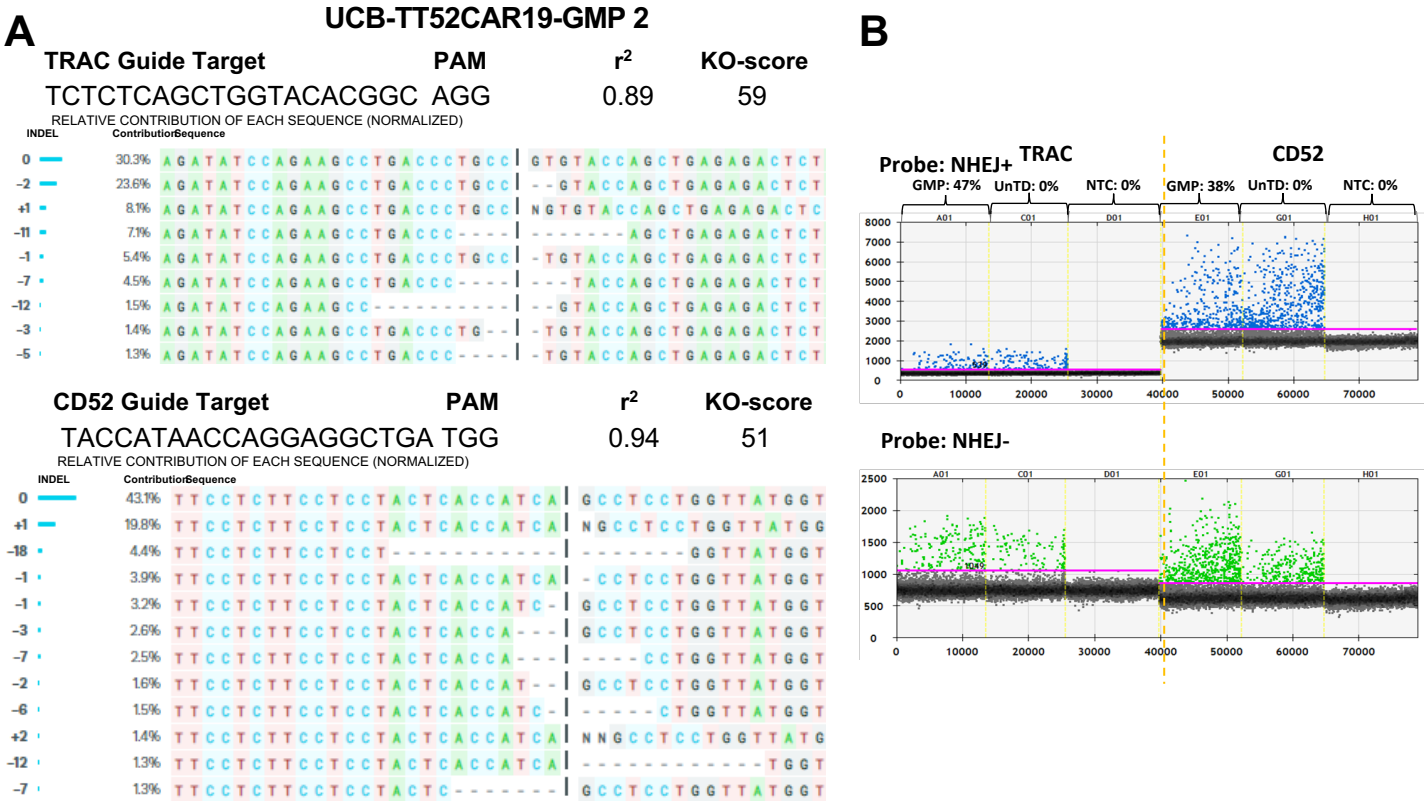

Supplementary Figure S4. Molecular characterisation of on-target events following CRISPR-Cas9 mediated cleavage. (A) ICE analysis of Sanger sequence traces identified indels in end of production UCB-TT52CAR19 GMP2 (UCB2) cells as signatures of NHEJ at the TRAC locus and at the CD52 target site. **(B)** Droplet Digital PCR (ddPCR) was used for the detection and quantification of indels by ddPCR at both the TRAC and CD52 sites using separate probes, one specific to the predicted NHEJ region ($NHEJ^{+}$) and a second outside the NHEJ region ($NHEJ^{-}$).

Supplementary Figure S5.

Top 10 IS Gene Names, Frequencies and Location

Rank	Gene Name	Frequency [%]	Location
Top1	VIPR2	0.185	7+159068479
Top2	NARF	0.077	17+82456875
Top3	TRAF2	0.068	9-136919938
Top4	PTBP2	0.068	1+96752542
Top5	PRRC2B	0.06	9+131411295
Top6	KIAA1715	0.057	2-175988556
Top7	UQCC3	0.057	11-62673431
Top8	MIR548AG1	0.057	4-59547877
Top9	MAML2	0.057	11-96065506
Top10	TNIK	0.057	3-171093835
#All Other mapp. IS	16853	99.257	

Seq Count 10 Strongest	880
Seq Count all other mapp. IS	117583
Total Seq Counts Used	118463

Supplementary Figure S5. Integration site analysis. Ligation-mediated PCR (LMPCR) detection and quantification of vector integration sites (IS) in UCB-TT52CAR19 GMP2 (UCB2) end of production cells where the top 10 most frequent sites comprised <0.1% of integrants.

Supplementary Figure S6.

A

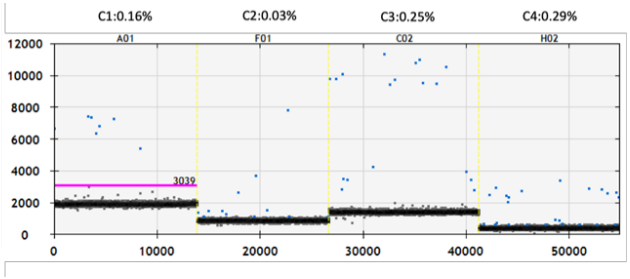

B

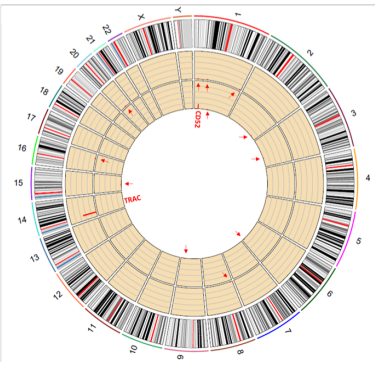

TRAC

Index	Chromosome	ChromStart	ChromEnd	Mutant Frequency
TRAC-01	chr14	23016465	23016487	50.58
TRAC-02	chr8	10627242	10627255	0.02
TRAC-03	chr1	68621798	68621815	0.11
TRAC-04	chr1	19612375	19612394	0.23
TRAC-05	chr1	242872248	242872256	0.02
TRAC-06	chr20	31622178	31622197	0.02
TRAC-07	chr16	66528021	66528030	0.05

CD52

Index	Chromosome	ChromStart	ChromEnd	Mutant Frequency
CD52-01	chr1	26644537	26644559	16.98
CD52-02	chr9	118431471	118431494	0.03
CD52-03	chr15	45497080	45497102	0.02
CD52-04	chr1	95875501	95875523	0.01
CD52-05	chr2	207739023	207739045	0.02
CD52-06	chr3	135905238	135905260	0.02
CD52-07	chr6	156954684	156954706	0.04

Supplementary Figure S6. Molecular characterisation of off-target and predicted translocation events following CRISPR-Cas9 mediated cleavage. (A) ddPCR based quantification of possible translocations after 'on-target' DNA scission. Low frequency translocation events (blue dots) C1-C4 arising between the edited TRAC and CD52 loci. Cumulative events for all four possible events were <1%. **(B)** Circos plot with verification of quantification using targeted NGS across six highest scoring predicted off-target sites. TRAC-01 (solid red line marking locus in outer yellow circle), CD52-01 (solid red line marking inner yellow circle) and at predicted off-target sites TRAC-02-TRAC-07 (red arrows marking outer yellow circle) and CD52-02-CD52-07 (red arrows marking inner yellow circle). Table shows that negligible off-target events were detected for both the TRAC and CD52 guides.

Supplementary Figure S7.

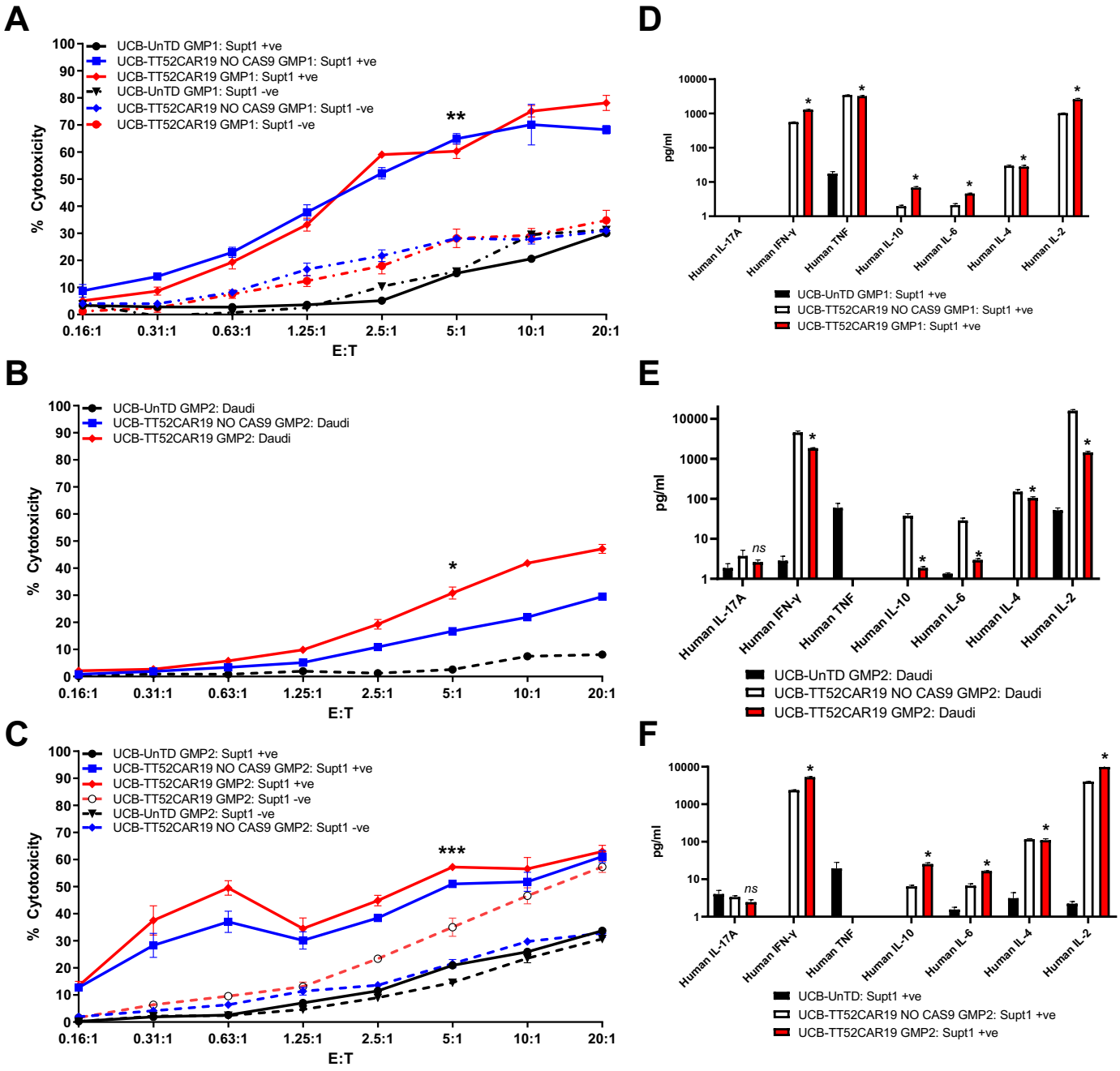

Supplementary Figure S7. *In vitro* killing potential and cytokine production of UCB-TT52CAR19 cells against CD19⁺ targets. In vitro cytotoxicity of UCB-TT52CAR19 cell banks compared to respective UCB-TT52CAR19 transduced but not edited (UCB-TT52CAR19 TCR⁺) or non-transduced (UnTD) controls when measured by ^{51}Cr chromium release of labelled Supt1 CD19⁺ or CD19⁻ cells **(A, C)** or CD19+ Daudi **(B)** cells following four hours co-culture at incremental effector (E) – target (T) ratio. Cell co-cultures ranged from 1 x 10^5 : 5 x 10^4 (at E:T of 20:1) to 8 x 10^2 : 5 x 10^4 (at E:T of 0.16:1). Effector responses were considered successful if ≥50% lysis was detected compared to UnTD controls at E:T cell ratios between 1.25:1 and 5:1. Error bars SEM, n=3 replicate/wells. *P<0.05, **P<0.01, ***P<0.001 by t-test. In vitro target specific cytokine secretion of UCB-TT52CAR19 GMP cell banks, and respective UCB-TT52CAR19 TCR⁺ or non-transduced (UnTD) controls at 1:1 E:T (1.25 x 10^5 of each effector and target cells) co-culture with Supt1 CD19⁺ cells **(D, F)** or CD19⁺ Daudi **(E)** cells overnight. The presence of cytokines in the co-culture supernatant was measured by cytokine bead array and levels >50pg/ml were considered positive responses. Significance was calculated between UCB-TT52CAR19 GMP1 and GMP2 banks and respective UnTD controls. *P<0.05 by t-test. Error bars represent SEM, n=3 replicates.

Supplementary Figure S8.

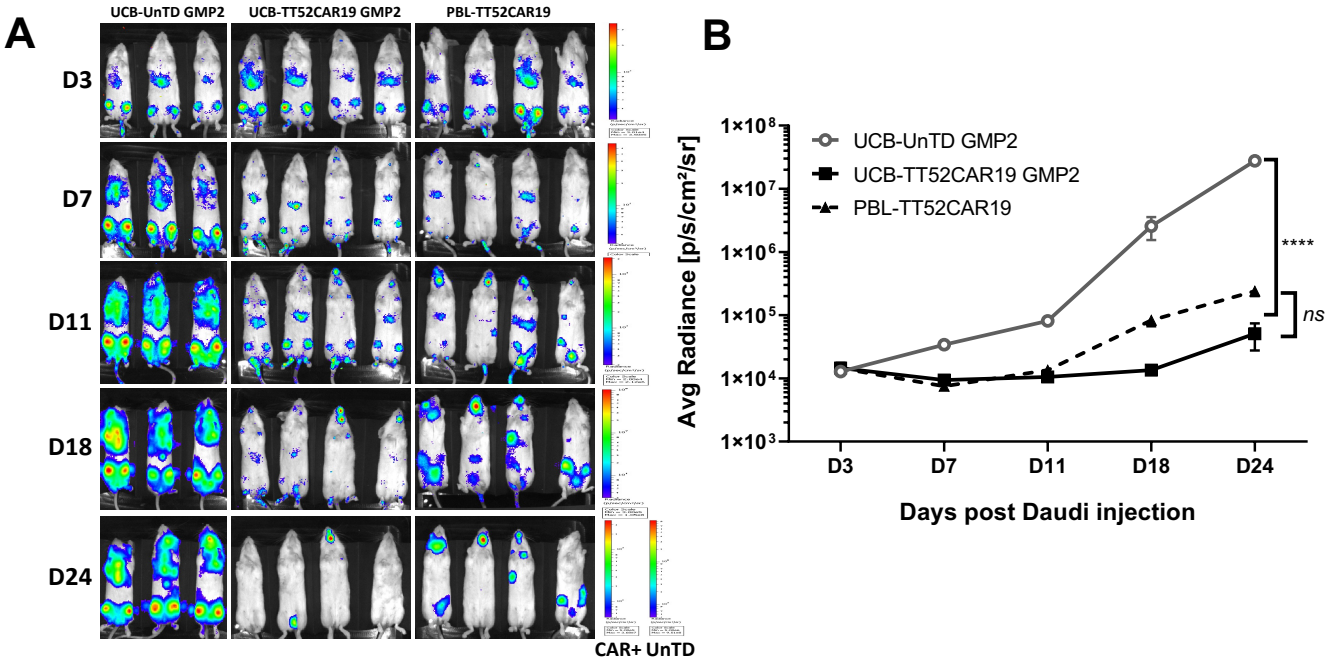

Supplementary Figure S8. *In vivo* tumour clearance in human:murine xenograft model of CD19⁺ disease.

Timeline of *in vivo* human:murine xenograft modelling indicating target and effector intravenous injection days and bioluminescent imaging (BLI) timepoints **(A)**. Serial measurement of bioluminescence of Daudi CD19⁺ B cell disease in immunodeficient mice NOD/SCID/γc (NSG) mice (n=12) infused with 5 x 10^5 GFP/luciferase expressing Daudi CD19⁺ B cells were treated on day 4 with either umbilical 5 x 10^6 cord blood (UCB) UCB-TT52CAR19 GMP2 (UCB2) (n=4) or peripheral blood lymphocyte (PBL) PBL-TT52CAR19 (n=4) and were monitored over a 4-week period **(B, C)** Non-transduced (UnTD) (n=3) T cells were used as controls. Error bars represent SEM. Significance compared by area under the curve using one-way ANOVA (F-value 10.63) with Tukey multiple comparison post-hoc; not significant (ns) $P \geq 0.05$; ****$P < 0.0001$.

Table S1.

UCB GMP1

HLA	A	B		Bw	C
Allele	02 : 01:01 24 : 02:01	07 : 02:01 15 : 01:01			03 : 03:01 07 : 02:01
HLA	DRB1	DRB3	DRB4	DRB5	DQB1
Allele	01 : 02:01 15 : 01:01			01 : 01:01	05 : 01:01 06 : 02:01
HLA	DPA1	DPB1			DQA1
Allele	01 : 03:01 02 : 01:01	04 : 01:01 11 : 01:01			01 : 01:02 01 : 02:01

UCB GMP2

HLA	A	B		Bw	C
Allele	01 : 01:01 25 : 01:01	07 : 02:01 08 : 01:01			07 : 01:01 07 : 02:01
HLA	DRB1	DRB3	DRB4	DRB5	DQB1
Allele	03 : 01:01 04 : 01:01	01 : 01:02	01 : 03:01		02 : 01:01 03 : 02:01
HLA	DPA1	DPB1			DQA1
Allele	01 : 03:01 :	04 : 01:01 :			03 : 01:01 05 : 01:01

Table S1. Umbilical Cord Blood unit tissue typing.
High-resolution Next Generation Sequencing tissue typing of UCB GMP1 and GMP2 batches.

Table S2.

Name	Application	Sequence	Primer/Probe
TRAC-on F	On- & off- targets NGS	CATGAGACCGTGACTTGCCA	Primer
TRAC-on R	On- & off- targets NGS	ACACATCAGAATCCTTACTTTGTGA	Primer
TRAC-02 F	On- & off- targets NGS	CAACTCTTGCTGCAACCTGA	Primer
TRAC-02 R	On- & off- targets NGS	TGCATCAGTCAACTTAGGTGAG	Primer
TRAC-03 F	On- & off- targets NGS	CCAAGATGGCAGAAGGGAAT	Primer
TRAC-03 R	On- & off- targets NGS	GAGGTCTTGCAAATTCAGGCT	Primer
TRAC-04 F	On- & off- targets NGS	AGCTTGAATGGCATCCTGAG	Primer
TRAC-04 R	On- & off- targets NGS	GCTTGGCCTCTCCAACTATG	Primer
TRAC-05 F	On- & off- targets NGS	CTGGAGGAAAGAAACAGACAGTAC	Primer
TRAC-05 R	On- & off- targets NGS	AAAAGGAGCCTGGCCATATTTC	Primer
TRAC-06 F	On- & off- targets NGS	CCGTCATCACACTGAACTTTGT	Primer
TRAC-06 R	On- & off- targets NGS	TCCCCATAACCTTTTCTGACCA	Primer
TRAC-07 F	On- & off- targets NGS	CACCCCAGCACCCACTATAC	Primer
TRAC-07 R	On- & off- targets NGS	GCCTCACAAGCAAGCCATAG	Primer
TRAC F	ddPCR NHEJ	TTGTCCATCACTGGCATC	Primer
TRAC R	ddPCR NHEJ	TGTGACACATTTGTTTGAGAATC	Primer
TRAC/NHEJ-	ddPCR NHEJ	TCATGTCCTAACCCTGATCCTCTTGT	Probe
TRAC/NHEJ+	ddPCR NHEJ	ACCCTGCCGTGTACCAGCT	Probe
CD52-on F	On- & off- targets NGS	CAAGACAGCCACGAAGAT	Primer
CD52-on R	On- & off- targets NGS	AGGAGAGAAGGCTGGGTC	Primer
CD52-02 F	On- & off- targets NGS	AGCCAGCCTACTTGCCAA	Primer
CD52-02 R	On- & off- targets NGS	CCCAGCTTCTTAGGAGTGTC	Primer
CD52-03 F	On- & off- targets NGS	GTGTGTAGACTTCAAAGGGCA	Primer
CD52-03 R	On- & off- targets NGS	ACTGGGTAATTCTGAGTTGTGG	Primer
CD52-04 F	On- & off- targets NGS	CTGGTTTCCTTGGAGCCA	Primer
CD52-04 R	On- & off- targets NGS	GTAGACCTGAGCCACCTGAC	Primer
CD52-05 F	On- & off- targets NGS	TTGCCTTACCACTGAGCT	Primer
CD52-05 R	On- & off- targets NGS	AGACAAGTGCTGCCTTACCA	Primer
CD52-06 F	On- & off- targets NGS	CTAGATATCCATGGGTGATTGG	Primer
CD52-06 R	On- & off- targets NGS	GACCCAGTTCACTTCCTGCT	Primer
CD52-07 F	On- & off- targets NGS	ATGCAAGAGTGGCCCAAAT	Primer
CD52-07 R	On- & off- targets NGS	TCACTTGTTCTCCCCTGACC	Primer
CD52 F	ddPCR NHEJ	CAAGACAGCCACGAAGAT	Primer
CD52 R	ddPCR NHEJ	AGGAGAGAAGGCTGGGTC	Primer
CD52/NHEJ-	ddPCR NHEJ	CCAAAGTTGCTTGGCATGGA	Probe
CD52/NHEJ+	ddPCR NHEJ	CATCAGCCTCCTGGTTATGGTACA	Probe
TRAC F + CD52 R	ddPCR Translocations	TTGTCCATCACTGGCATC	Primer F
TRAC F + CD52 R	ddPCR Translocations	GCCAGGCGTTGCTCTTAC	Primer R
CD52 F + TRAC R	ddPCR Translocations	CAAGACAGCCACGAAGAT	Primer F
CD52 F + TRAC R	ddPCR Translocations	TGTGACACATTTGTTTGAGAATC	Primer R
TRAC R + CD52 R	ddPCR Translocations	TCAGAATCCTTACTTTGTGACAC	Primer F
TRAC R + CD52 R	ddPCR Translocations	GCCAGGCGTTGCTCTTAC	Primer R
CD52 F + TRAC F	ddPCR Translocations	CAAGACAGCCACGAAGAT	Primer F
CD52 F + TRAC F	ddPCR Translocations	ATCACTGGCATCTGGACTC	Primer R
TRAC F + CD52 R	ddPCR Translocations	TCATGTCCTAACCCTGATCCTCTTGT	Probe
CD52 F + TRAC R	ddPCR Translocations	AGTCTGTCTGCCTATTCACCGATT	Probe
TRAC R + CD52 R	ddPCR Translocations	TCGGTGAATAGGCAGACAGACTTGT	Probe
CD52 F + TRAC F	ddPCR Translocations	TGGGACAAGAGGATCAGGGT	Probe
Albumin F	ddPCR Translocations	GCTGCTATCTCTTGTGGGCTGT	Primer
Albumin R	ddPCR Translocations	ACTCATGGGAGCTGCTGGTTC	Primer
Albumin	ddPCR Translocations	CCTGTCATGCCCACACAAATCTCTCC	Probe

Table S2. On-, off-target and translocation primer and probe sets.
Primer and probe sets used for quantification of 'on-target' and 'off-target' NHEJ events or possible translocations after 'on-target' DNA scission in UCB-TT52CAR19 Good Manufacturing Process (GMP) batches GMP1 (UCB1) and GMP2 (UCB2).

Table S3.

	UCB1	UCB2
	Cell counts in fresh UCB unit	
Total WBC	1234 x 10^6	822 x 10^6
Lymphocyte	438 x 10^6	418 x 10^6
	Cell counts post CD62L$^+$ selection	
Total WBC	184 x 10^6	118 x 10^6
Lymphocyte	133 x 10^6	96 x 10^6

Table S3. Umbilical Cord Blood (UCB) cell counts pre or post CD62L+ selection. White blood cell (WBC) and lymphocyte Sysmex counts in fresh UCB units pre and post machine-based CD62L+ selection.